2007

Cell Wall Proteome in the Maize Primary Root Elongation Zone. II. Region-Specific Changes in Water Soluble and Lightly Ionically Bound Proteins under Water Deficit1[W][OA]

Jinming Zhu
University of Missouri- Columbia

Sophie Alvarez
Utah State University- Logan

Ellen L. Marsh
Utah State University- Logan, emarsh2@unl.edu

Mary E. LeNoble
University of Missouri- Columbia

In-Jeong Cho
University of Missouri- Columbia

See next page for additional authors

Cell Wall Proteome in the Maize Primary Root Elongation Zone. II. Region-Specific Changes in Water Soluble and Lightly Ionically Bound Proteins under Water Deficit[1][W][OA]

Jinming Zhu[2], Sophie Alvarez[2,3], Ellen L. Marsh, Mary E. LeNoble, In-Jeong Cho, Mayandi Sivaguru[4], Sixue Chen[3], Henry T. Nguyen, Yajun Wu, Daniel P. Schachtman, and Robert E. Sharp*

Division of Plant Sciences (J.Z., M.E.L., I.-J.C., H.T.N., R.E.S.) and Molecular Cytology Core (M.S.), University of Missouri, Columbia, Missouri 65211; Donald Danforth Plant Science Center, St. Louis, Missouri 63132 (S.A., E.L.M., S.C., D.P.S.); and Department of Plants, Soils and Climate, Utah State University, Logan, Utah 84322 (Y.W.)

Previous work on the adaptation of maize (*Zea mays*) primary roots to water deficit showed that cell elongation is maintained preferentially toward the apex, and that this response involves modification of cell wall extension properties. To gain a comprehensive understanding of how cell wall protein (CWP) composition changes in association with the differential growth responses to water deficit in different regions of the elongation zone, a proteomics approach was used to examine water soluble and loosely ionically bound CWPs. The results revealed major and predominantly region-specific changes in protein profiles between well-watered and water-stressed roots. In total, 152 water deficit-responsive proteins were identified and categorized into five groups based on their potential function in the cell wall: reactive oxygen species (ROS) metabolism, defense and detoxification, hydrolases, carbohydrate metabolism, and other/unknown. The results indicate that stress-induced changes in CWPs involve multiple processes that are likely to regulate the response of cell elongation. In particular, the changes in protein abundance related to ROS metabolism predicted an increase in apoplastic ROS production in the apical region of the elongation zone of water-stressed roots. This was verified by quantification of hydrogen peroxide content in extracted apoplastic fluid and by in situ imaging of apoplastic ROS levels. This response could contribute directly to the enhancement of wall loosening in this region. This large-scale proteomic analysis provides novel insights into the complexity of mechanisms that regulate root growth under water deficit conditions and highlights the spatial differences in CWP composition in the root elongation zone.

Roots often continue to grow under water deficits that completely inhibit shoot and leaf elongation (Sharp and Davies, 1979; Westgate and Boyer, 1985), and this is considered an important mechanism of plant adaptation to water-limited conditions (Sharp and Davies, 1989). Investigation of the mechanisms of root growth adaptation to water deficit is important for improving plant performance under drought, because water resources for agriculture are becoming increasingly limited.

The physiology of maize (*Zea mays*) primary root elongation at low water potentials has been studied extensively (for review, see Sharp et al., 2004), which has provided the foundation for an understanding of the complex network of responses involved. Analysis of the relative elongation rate profile within the root elongation zone showed that under severe water deficit, elongation rates are fully maintained in the apical few millimeters but progressively inhibited as cells are displaced further from the root apex (Sharp et al., 1988; Liang et al., 1997). To help understand the maintenance of elongation in the apical region of roots growing under water deficit conditions, Spollen and Sharp (1991) measured the spatial distribution of turgor pressure and found that values were uniformly decreased by over 50% throughout the elongation zone of water-stressed compared to well-watered roots. These results suggested that water stress results in an increase in longitudinal cell wall extensibility in the apical region, which was confirmed by direct measurement of

[1] This work was supported by the National Science Foundation, Plant Genome Program (grant no. DBI–0211842), the Missouri Agricultural Experiment Station (project no. MO–PSFC0355), and the Utah Agricultural Experiment Station (project no. UTA 000366).

[2] These authors contributed equally to the article.

[3] Present address: Department of Botany, University of Florida, Gainesville, FL 32610.

[4] Present address: Institute for Genomic Biology, University of Illinois at Urbana-Champaign, Urbana, IL 61801.

* Corresponding author; e-mail sharpr@missouri.edu.

The author responsible for distribution of materials integral to the findings presented in this article in accordance with the policy described in the Instructions for Authors (www.plantphysiol.org) is: Robert E. Sharp (sharpr@missouri.edu).

[W] The online version of this article contains Web-only data.

[OA] Open Access articles can be viewed online without a subscription.

www.plantphysiol.org/cgi/doi/10.1104/pp.107.107250

acid-induced extension (Wu et al., 1996). In contrast, cell wall extension properties are inhibited in the basal region of the elongation zone in water-stressed compared to well-watered roots (Wu et al., 1996; Fan and Neumann, 2004; Fan et al., 2006). Additional studies with the same experimental system demonstrated that activities of two cell wall proteins (CWPs) with known or proposed wall loosening properties, expansins, and xyloglucan endotransglucosylase/hydrolase (XTH), were increased specifically in the apical few millimeters of water-stressed compared to well-watered roots (Wu et al., 1994, 1996), providing a biochemical basis for the increase in cell wall extensibility (Wu and Cosgrove, 2000). At the transcript level, three expansin genes were up-regulated in the apical region and down-regulated in the basal region of the elongation zone of water-stressed roots, correlating with the increase and decrease of extensibility in these regions, respectively (Wu et al., 2001).

Since cell wall extensibility changes are likely to involve multiple components and processes, the previous work provided a limited understanding of the cell wall biology of root growth regulation under water deficits. In this study, a proteomics approach was used to expand our understanding of the CWPs that change in abundance in the elongation zone of water-stressed roots. By combining spatial analysis of the CWP changes with knowledge of the elongation rate patterns we aimed to gain further insight into the CWPs that are potentially involved in controlling the responses of cell elongation.

Proteomics approaches are increasingly being applied to identify large numbers of proteins from cell walls (Robertson et al., 1997; Blee et al., 2001; Chivasa et al., 2002; Watson et al., 2004; Bayer et al., 2006; Zhu et al., 2006). However, to our knowledge, no cell wall proteomics studies have focused on the involvement of CWPs in the response of root growth to water deficit conditions. Various methods have been developed to extract CWP fractions that may be loosely to very tightly bound to the cell wall matrix (Fry, 1988). The fraction 1 CWPs described in this study represent those proteins that are soluble in apoplastic fluid or lightly ionically bound to the cell walls. Proteomic studies of fraction 1 CWPs have been performed in leaves of several species (Haslam et al., 2003; Boudart et al., 2005), including a study of tobacco (*Nicotiana tabacum*) in which it was shown that 20 fraction 1 CWPs changed in abundance in response to salt stress (Dani et al., 2005). These studies not only revealed very different protein compositions in different species, but also reflected the variety of functions of fraction 1 CWPs.

In a previous study, an infiltration and centrifugation method was optimized for the extraction of fraction 1 CWPs from the elongation zone of the maize primary root with minimal cytosolic protein contamination (Zhu et al., 2006). In this study, this method was used to gain a more comprehensive understanding of how the composition of fraction 1 CWPs changes in association with the differential responses of cell elongation to water deficit in different regions of the elongation zone. The results reveal major and predominantly region-specific changes in protein profiles between well-watered and water-stressed roots that provide novel insights into the processes involved in regulating the root growth response to water stress.

RESULTS

Two-Dimensional Gel Analysis of Water Deficit-Responsive Fraction 1 CWPs in Different Regions of the Root Elongation Zone

Fraction 1 CWPs were extracted from four contiguous regions within the apical 20 mm of the primary root of maize seedlings grown under well-watered or water-stressed conditions. As shown in Figure 1, relative elongation rates were completely maintained under water deficit in the apical 3 mm region (R1); the 3 to 7 mm region (R2) exhibited maximum elongation rates in well-watered roots but progressive inhibition of elongation under water deficit; in the 7 to 12 mm region (R3), elongation decelerated in well-watered roots and was completely inhibited under water deficit; the 12 to 20 mm region (R4) was nonelongating in both well-watered and water-stressed roots. Two well-watered controls were collected, a temporal control in which well-watered roots were harvested at the same time as the water-stressed roots (48 h after transplanting), and a developmental control in which well-watered roots were harvested at 24 h after transplanting when they had reached the same length as the

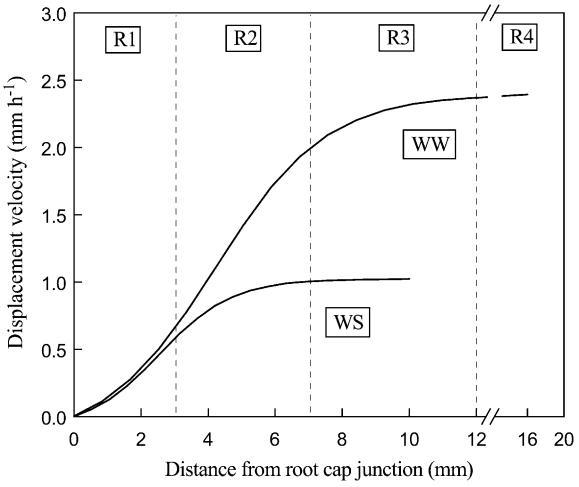

Figure 1. Displacement velocity as a function of distance from the root cap junction of primary roots of maize 'FR697' at 48 h after transplanting to well-watered (WW; water potential of −0.03 MPa) or water-stressed (WS; water potential of −1.6 MPa) conditions. Local elongation rates are obtained from the derivative of velocity with respect to position. R1 to R4, as harvested for CWP extraction in this study, are indicated. The velocity curves are reproduced from Sharp et al. (2004) with permission from Oxford University Press; the original data were calculated from root elongation rates and cortical cell length profiles.

water-stressed roots. The two controls were important to help identify proteins that showed true change in abundance in response to water stress, because the protein composition might also vary with root development under well-watered conditions. Previous work in a different cultivar showed that the spatial pattern of relative elongation rate was almost identical in the two well-watered controls (Liang et al., 1997).

The extracted CWPs were separated by two-dimensional electrophoresis (2-DE) and stained with SyproRuby. Despite the large number of roots used for CWP extraction (750 roots per sample), very low amounts of protein were available for this analysis due both to the extremely small proportion of total cellular proteins comprised by the extracted fraction 1 CWPs (approximately 0.01%), as well as the small regions of the root from which the proteins were extracted. However, the extraction procedure provided a relatively uncomplicated protein fraction, making these samples ideal for gel analysis. Furthermore, even though the total amount of protein loaded on each gel was low, individual proteins could be visualized because of the relatively small numbers of proteins in the extracts. On average, 157 spots were visualized from gels containing protein from R1, 340 from R2, 384 from R3, and 224 from R4. Representative 2-DE gel images for each region of each treatment are shown in Figure 2; gel images of replicate samples were closely comparable in spot patterns and intensity.

To be considered in our within-region analyses, protein spots needed to be present (or absent) in all three replicate gels in a specific region of each treatment. This approach allowed analysis in specific regions of proteins that did not necessarily yield reproducible results in one or more other regions. For R1 to R3, the numbers of spots that were reproducibly present in one or more treatments are shown in Figure 3. The results of the gel analysis are not shown for R4 because this was outside of the elongation zone in both well-watered and water-stressed roots (Fig. 1). However, R4 was used for abundance analysis of proteins that were stress responsive in one or more of the other regions (see below). In each region, the greatest proportion of spots was common to all treatments, while the two well-watered controls consistently had more spots in common with each other than with the water-stressed roots. In R1, 34 protein spots were found in both well-watered controls but not in the water-stressed roots and five were unique to the water-stressed roots (Fig. 3), suggesting that under water stress the 34 proteins are down-regulated to very low levels and the five proteins are induced from an undetectable level. Of the 58 spots that were common to the water-stressed roots and to both (52 spots) or only one (six spots) of the well-watered controls, the abundance of 19 significantly increased and 10 significantly decreased under water stress. It should be noted that all six of the spots that were found in the water-stressed roots but in only one of the controls were up-regulated rather than down-regulated by water stress. Since these spots were undetectable in the other control, they were considered to be reproducibly up-regulated by water stress. This was also true for all such spots in R2 and R3. In R2, 22 protein spots were found in both well-watered controls and not in the water-stressed roots, 18 were unique to water-stressed roots, and of 150 spots common to the stressed roots and to one or both controls, the abundance of 14 increased and 17 decreased under water stress. In R3, 32 spots were found in both well-watered controls but not under water stress, nine were unique to the water-stressed roots, and of 197 spots common to the stressed roots and to one or both controls, the abundance of 26 increased and 23 decreased under water stress (Fig. 3). In proportion to the total number of proteins found in each region, the largest percentage change in protein abundance in water-stressed compared to well-watered roots was found in R1.

The changes in abundance of CWPs due to water deficit in R1, R2, and R3 were predominantly region specific. When the stress-responsive protein spots were compared by spot matching across the regions, 44 of the 68 spots in R1, 48 of the 71 spots in R2, and 57 of the 90 spots in R3 were responsive only in those specific regions (Fig. 4). Only 12 protein spots were stress responsive in all three regions. The large number of region-specific changes in protein abundance in response to water stress emphasizes the importance and effectiveness of the spatial analysis approach that we used to study the CWPs in the root elongation zone.

Identification of the Water Deficit-Responsive Fraction 1 CWPs

The proteins whose abundance changed significantly in response to water deficit in R1, R2, and/or R3 were excised and identified using mass spectrometry. The protein identifications are shown in Supplemental Table S1; confident identifications were based on multiple peptide matches and significant Mascot scores. Fifty three, 49, and 63 proteins were identified from the 68, 71, and 90 water deficit-responsive protein spots in R1, R2, and R3, respectively (Fig. 3). In most cases, each protein spot was identified as a single protein; those spots that yielded more than one confident identification are marked with an asterisk in Supplemental Table S1. From 122 spots identified by mass spectrometry, 152 different proteins were identified. As shown in Supplemental Table S1, most of the proteins (85%) were identified from one region of the root only. In other cases, proteins were identified in two (5%) or three (2%) regions. A few proteins (8%) were identified by cross comparison with master gels that were established from fraction 1 CWPs of the elongation zone of well-watered roots (Zhu et al., 2006). The success rate for protein reidentification from more than one region was 95% for spots with comparable locations on the gels. It should be noted that for some protein spots (e.g. spots 194, 216, 1230, 3426, 3502)

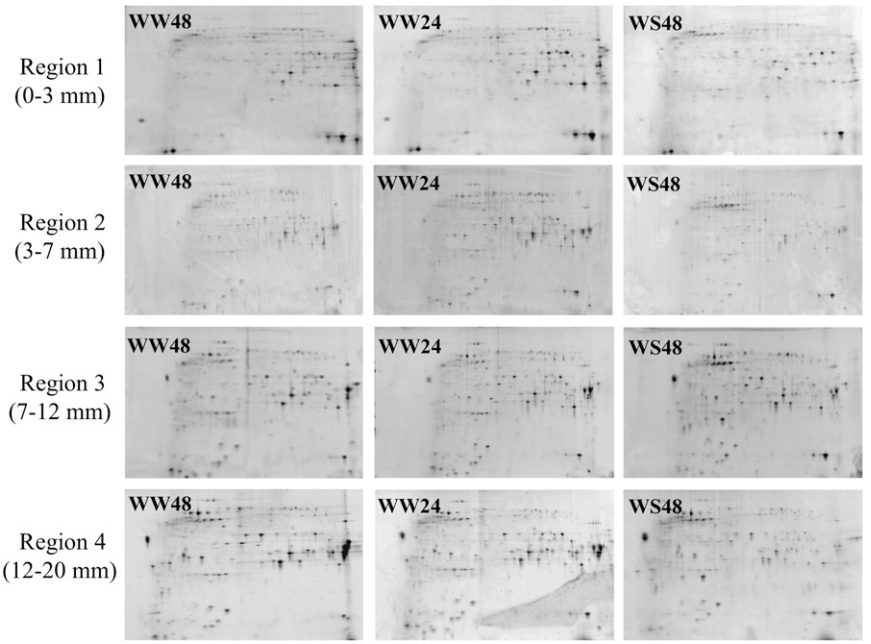

Figure 2. Representative two-dimensional SDS-PAGE gel images for water soluble and lightly ionically bound (fraction 1) CWPs extracted from R1 to R4 of well-watered roots at 48 h (WW48; temporal control, roots of the same age as water-stressed roots) and 24 h (WW24; developmental control, roots of the same length as water-stressed roots) after transplanting, and water-stressed roots at 48 h after transplanting (WS48). Three replicates were analyzed for each treatment.

there was a discrepancy between the observed and expected M_r, which may be the result of protein modification, incomplete genome/protein databases for maize, or alternate splicing products (Sun et al., 2005). Also, the identification of the same protein from different spots (e.g. spots 141, 142, 150, 402) indicates possible protein isoforms for which posttranslational modifications may have occurred, or these may be isoforms that arise from multigene families. The complete data is accessible at http://rootgenomics.missouri.edu/proticdb-1.2.1/Protic/home. To display these data we used the PROTICdb database (Ferry-Dumazet et al., 2005).

A large number of the proteins for which we found water stress-induced changes in abundance are known to be localized in cell walls, including two putative oxalate oxidases and two probable germin protein 4s, one α-L-arabinofuranosidase, one α-1,4-glucan-protein synthase, two β-galactosidases, two putative chitinases, three endo-1,3;1,4-β-D-glucanases, three putative α-galactosidase preproteins, four β-1,3-glucanases, five XTHs, four xylosidases, 12 β-D-glucosidases, and 18 peroxidases. In addition, most of the identified proteins (69%) have a putative N-terminal signal peptide that may lead to protein targeting into the secretory pathway (Nielsen et al., 1997), and 11% were predicted to be nonclassical secretory proteins that may be targeted to cell walls using an alternative pathway (Bendtsen et al., 2004; Supplemental Table S1). It should be noted that expansins, which were shown previously to exhibit altered activity and gene expression in the maize primary root elongation zone under water deficit (Wu et al., 1996, 2001), were not identified. Expansins are tightly bound to the cell wall and are not expected to be present in fraction 1 CWP extracts (McQueen-Mason et al., 1992).

Functional Classification and Region Specificity of Water Deficit-Responsive Fraction 1 CWPs

To better understand the biological processes encompassed by the identified proteins, the proteins were classified in five categories based on their annotations and potential functions in the cell wall (Supplemental Table S1). Of the 152 proteins identified from R1 to R3, 30 were categorized as being involved in reactive oxygen species (ROS) metabolism, 35 were in the category of defense and detoxification, 39 were related to hydrolase activity, 17 were related to carbohydrate metabolism, and 31 were considered as other/unknown. Within each functional category, changes in protein abundance in water-stressed compared to well-watered roots are shown for R1 to R3 in Figures 5 to 9. To allow for quantitative comparisons between the proteins, the data are expressed as fold-change values ($\log_{10}$ scale) using mean values from the two well-watered controls and a background value of 0.001 when a protein spot could not be visualized in a particular treatment. For spots that yielded multiple identifications (Supplemental Table S1), only the most confident identification is presented in Figures 5 to 9.

Because the root elongation zone was shorter in the water-stressed roots (Fig. 1), some of the changes in protein abundance observed in R2 and R3 of water-stressed compared to well-watered roots could be attributed to the differences in stage of cell development between the treatments rather than to specific responses to water stress. Thus, stress-responsive proteins in R2 (decelerating region under stress) and R3 (initial nongrowing region under stress) were also compared to R3 and R4, respectively, in well-watered roots, which exhibited comparable developmental stages. Changes in protein abundance in R2 under

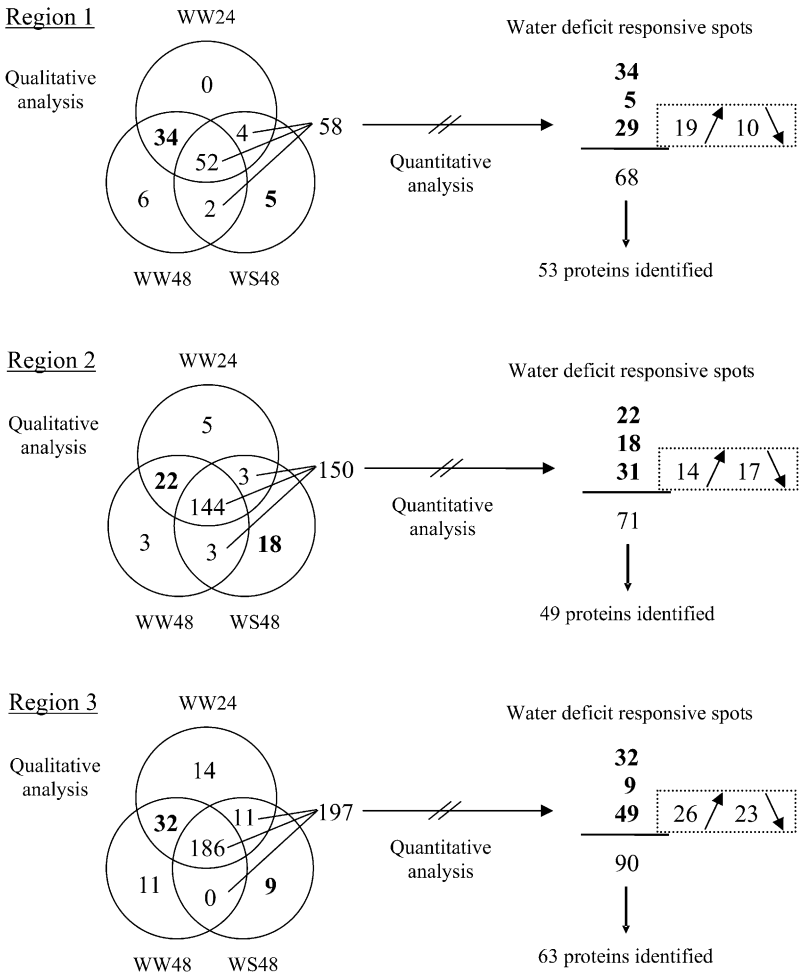

Figure 3. Qualitative and quantitative analysis of changes in abundance of fraction 1 CWPs from R1 to R3 of water-stressed roots (WS48) compared to well-watered temporal (WW48) and developmental (WW24) controls. The numbers of water deficit-responsive proteins are indicated, including those unique to well-watered or water-stressed roots and those that significantly increased or decreased in abundance under water stress.

water stress that were consistent when compared to both well-watered R2 and R3 were considered to be independent of the shortening of the elongation zone; such proteins are marked with an asterisk in Figures 5 to 9. Similarly, consistent responses in water-stressed R3 when compared to well-watered R3 and R4 were considered to be independent of the change in developmental stage. Since elongation rates were the same in R1 under well-watered and water-stressed conditions, all changes in protein abundance between the stressed and well-watered treatments in R1 were considered to be specific responses to water stress.

In all functional categories, the changes in abundance of CWPs due to water deficit were predominantly region specific (Figs. 5–9). Where the same protein was stress responsive in more than one region, the direction of the response (increase or decrease in abundance) was the same in most cases, although there were several exceptions where proteins exhibited opposite responses in different, and sometimes adjacent, regions.

Changes in CWP abundance under water deficit in the category of ROS metabolism are shown in Figure 5. Of the 20 proteins identified in this category from R1 to R3, a greater number exhibited increases rather than decreases in abundance in R1 and R2. The abundance of one superoxide dismutase [Cu-Zn], one putative oxalate oxidase, one probable germin protein, and three peroxidases increased in R1. The putative oxalate oxidase was consistently more abundant throughout the three regions, whereas the other proteins increased in abundance in R1 specifically. In R3, a greater number of proteins decreased rather than increased in abundance in the stressed roots, although the abundance of a different putative oxalate oxidase (same accession number but different spot) and a putative peroxidase increased greatly.

Of the 26 proteins in the category of defense and detoxification, a majority exhibited decreases in abundance in water-stressed compared to well-watered roots in R1, R2, and R3 (Fig. 6). In the category of hydrolases, in which a total of 33 stress-responsive proteins were identified, 13 of the 18 proteins in R1 exhibited a decrease in abundance under water stress (Fig. 7). These responses, including two XTHs and two endo-1,3;1,4-β-D-glucanases, were specific to R1, with the exception of another XTH (spot 190) that decreased in abundance in all three regions. A fourth XTH (spot 1,650) exhibited a small increase in abundance specifically in

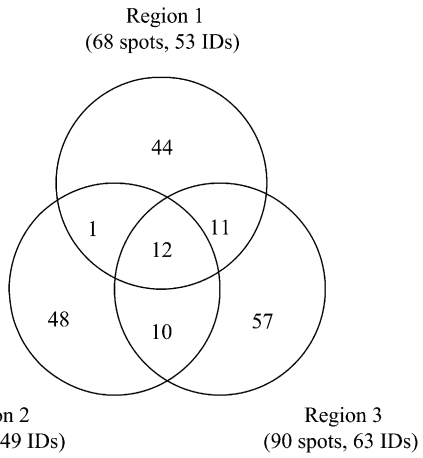

Figure 4. Distribution among R1 to R3 of water deficit-responsive fraction 1 CWPs, showing that the changes in protein abundance in water-stressed compared to well-watered roots were predominantly region specific.

R2, although this change was likely attributable to the change in developmental profile. All five of the proteins in the hydrolase category that increased in abundance in R1 of the water-stressed roots were identified as β-D-glucosidases. Four of these proteins also increased in abundance in R2 and R3.

There were 10 stress-responsive proteins identified in the category of carbohydrate metabolism (Fig. 8), of which five of the six proteins in R1 and R2 decreased in abundance, whereas four of nine increased in abundance in R3. Notably, all three soluble acid invertases increased in abundance in R2 or R3. There were 21 proteins in the category of other/unknown (Fig. 9). Most of these proteins (19 out of 21) showed region-specific responses to water stress. For example, a α-1, 4-glucan-protein synthase increased in abundance only in R1, and two legumin-like proteins increased in abundance only in R2.

Spatial Distribution of Fraction 1 CWPs in Well-Watered and Water-Stressed Roots

To reveal the spatial distribution of abundance along the elongation zone of the water deficit-responsive proteins, gel images of all regions of all treatments were normalized, which allowed for across-region comparisons of protein abundance. Only those protein spots that were reproducibly present (or absent) in all three replicates in all regions of all treatments were selected for this analysis, restricting the analysis to 73 of the 110 proteins for which fold-change responses are presented in Figures 5 to 9. The results are shown in Figure 10 and Supplemental Figures S1 to S5.

The abundance profiles along the elongation zone varied greatly for the different proteins both within and between protein families as well as between the well-watered and water-stressed treatments (in general the profiles were very similar in the two well-watered controls). As an example of the diversity within a protein family, the spatial distributions of

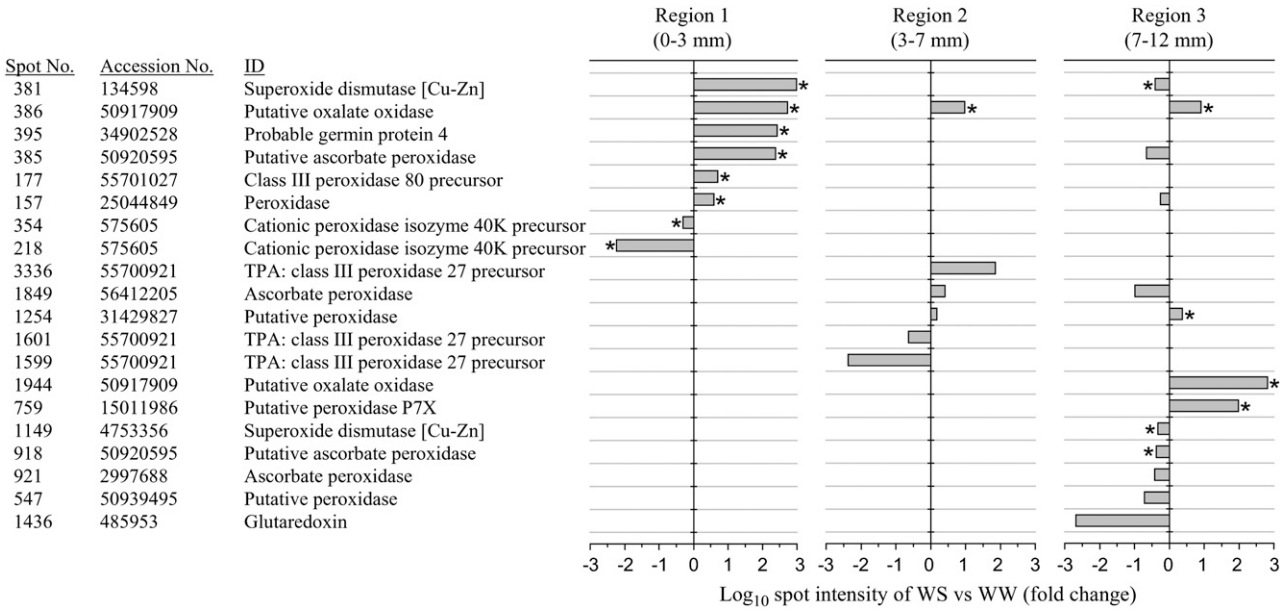

Spot No.	Accession No.	ID
381	134598	Superoxide dismutase [Cu-Zn]
386	50917909	Putative oxalate oxidase
395	34902528	Probable germin protein 4
385	50920595	Putative ascorbate peroxidase
177	55701027	Class III peroxidase 80 precursor
157	25044849	Peroxidase
354	575605	Cationic peroxidase isozyme 40K precursor
218	575605	Cationic peroxidase isozyme 40K precursor
3336	55700921	TPA: class III peroxidase 27 precursor
1849	56412205	Ascorbate peroxidase
1254	31429827	Putative peroxidase
1601	55700921	TPA: class III peroxidase 27 precursor
1599	55700921	TPA: class III peroxidase 27 precursor
1944	50917909	Putative oxalate oxidase
759	15011986	Putative peroxidase P7X
1149	4753356	Superoxide dismutase [Cu-Zn]
918	50920595	Putative ascorbate peroxidase
921	2997688	Ascorbate peroxidase
547	50939495	Putative peroxidase
1436	485953	Glutaredoxin

Figure 5. Responses to water stress (WS) in R1 to R3 of fraction 1 CWPs in the category of ROS metabolism. To allow quantitative comparisons between the proteins, the data are expressed as fold-change values ($\log_{10}$ scale) using mean values from the two well-watered (WW) controls and a background value of 0.001 when a protein spot was not visualized in a particular treatment. The changes in protein abundance that are marked with an asterisk are considered to be independent of developmental changes associated with the stress-induced shortening of the elongation zone (Fig. 1) and, therefore, likely to be specific responses to water stress (see text for details of this analysis).

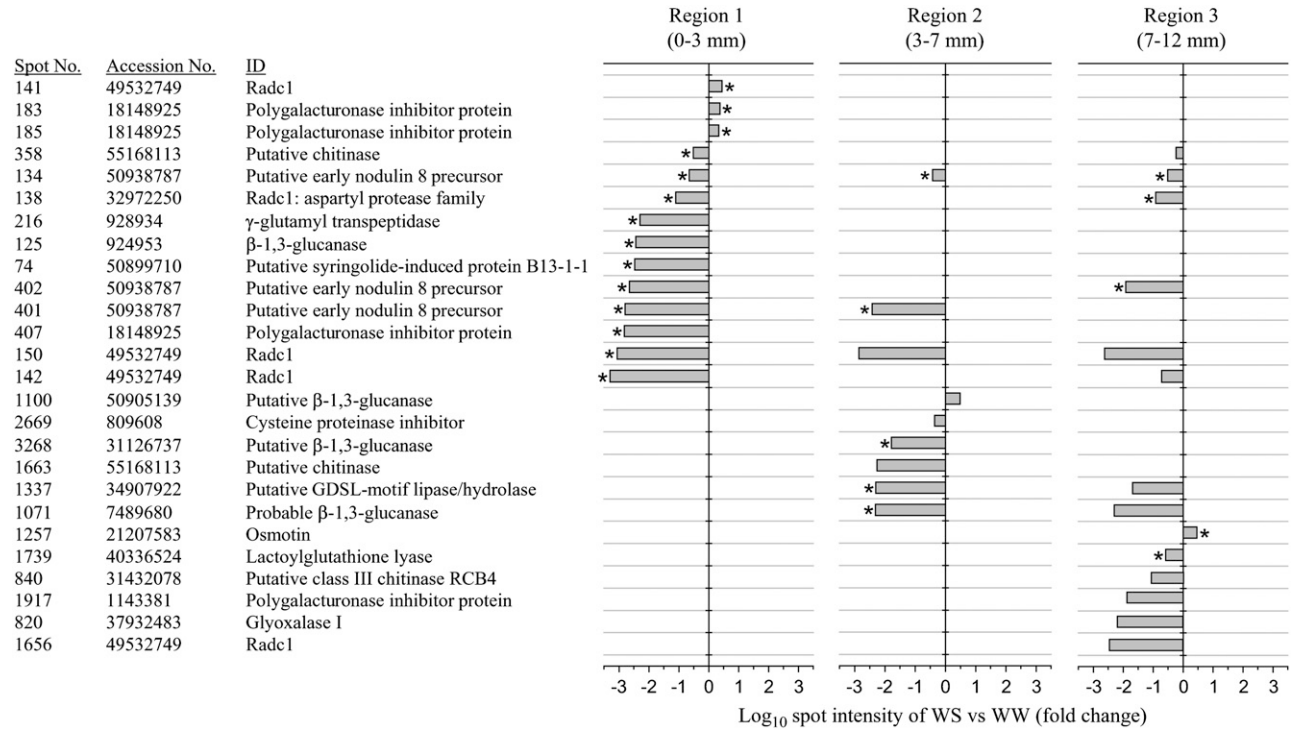

Spot No.	Accession No.	ID
141	49532749	Radc1
183	18148925	Polygalacturonase inhibitor protein
185	18148925	Polygalacturonase inhibitor protein
358	55168113	Putative chitinase
134	50938787	Putative early nodulin 8 precursor
138	32972250	Radc1: aspartyl protease family
216	928934	γ-glutamyl transpeptidase
125	924953	β-1,3-glucanase
74	50899710	Putative syringolide-induced protein B13-1-1
402	50938787	Putative early nodulin 8 precursor
401	50938787	Putative early nodulin 8 precursor
407	18148925	Polygalacturonase inhibitor protein
150	49532749	Radc1
142	49532749	Radc1
1100	50905139	Putative β-1,3-glucanase
2669	809608	Cysteine proteinase inhibitor
3268	31126737	Putative β-1,3-glucanase
1663	55168113	Putative chitinase
1337	34907922	Putative GDSL-motif lipase/hydrolase
1071	7489680	Probable β-1,3-glucanase
1257	21207583	Osmotin
1739	40336524	Lactoylglutathione lyase
840	31432078	Putative class III chitinase RCB4
1917	1143381	Polygalacturonase inhibitor protein
820	37932483	Glyoxalase I
1656	49532749	Radc1

Figure 6. Responses to water stress in R1 to R3 of fraction 1 CWPs in the category of defense and detoxification. See the legend of Figure 5 for full description.

abundance of nine β-D-glucosidases are presented in Figure 10. Spot 355 and 400 showed expression only in R1, and moreover exhibited opposite stress responses with spot 355 decreasing in abundance under water deficit while spot 400 increased in abundance. Spots 1041 and 3514 were mainly present only in R2, and also showed opposite responses to water deficit with spot 1041 decreasing and spot 3514 increasing in abundance. Spot 409 was expressed in R2 and R3 of well-watered roots and increased in abundance in R1, R2, and R3 of water-stressed roots. Spot 3502 was expressed in R3 and R4 of well-watered roots, but the expression shifted to R2 in water-stressed roots. Spots 97, 99, and 305 were expressed in all four regions of well-watered roots with a gradual increase in abundance with increasing distance from the root apex. Water deficit caused a large increase in abundance of these proteins in R1 to R3, with the highest abundance occurring in R2 in each case. This example highlights the spatial complexity of the growth zone of maize roots and may also suggest differences in function between members of this large gene family.

Increase in Apoplastic ROS in R1 of Water-Stressed Roots

As detailed above, several of the CWPs whose abundance increased in R1 of the water-stressed roots were classified as being involved in ROS metabolism (Fig. 5), suggesting that the amount of apoplastic ROS may have been altered. In particular, the increased abundance of superoxide dismutase and of two putative oxalate oxidase/germin proteins suggested that the production of hydrogen peroxide (H_2O_2) may be greater in this region of water-stressed compared to well-watered roots.

Two methods were used to evaluate the prediction from the proteomic data of increased apoplastic ROS levels in R1 of water-stressed roots. First, H_2O_2 content was measured in apoplastic fluid extracted from R1 of well-watered and water-stressed roots using the same procedures used to extract the CWPs. The results showed that the apoplastic H_2O_2 content doubled in the water-stressed roots (Fig. 11). Since the extracts from the water-stressed roots had increased abundance of peroxidases (Fig. 5), additional experiments were conducted to assess whether differences in peroxidase activity may have differentially affected the H_2O_2 quantification between the treatments. The extracts from the water-stressed roots indeed had higher peroxidase activities compared to those from well-watered roots (data not shown). However, the estimated consumption of H_2O_2 by peroxidase activity represented only a small fraction of the H_2O_2 content of the extracts, and would not have appreciably affected the H_2O_2 measurements.

Measurements of ROS can be variable under different conditions and with different methods (Tarpey and Fridovich, 2001). Accordingly, to verify the finding of increased apoplastic H_2O_2 in R1 of water-stressed

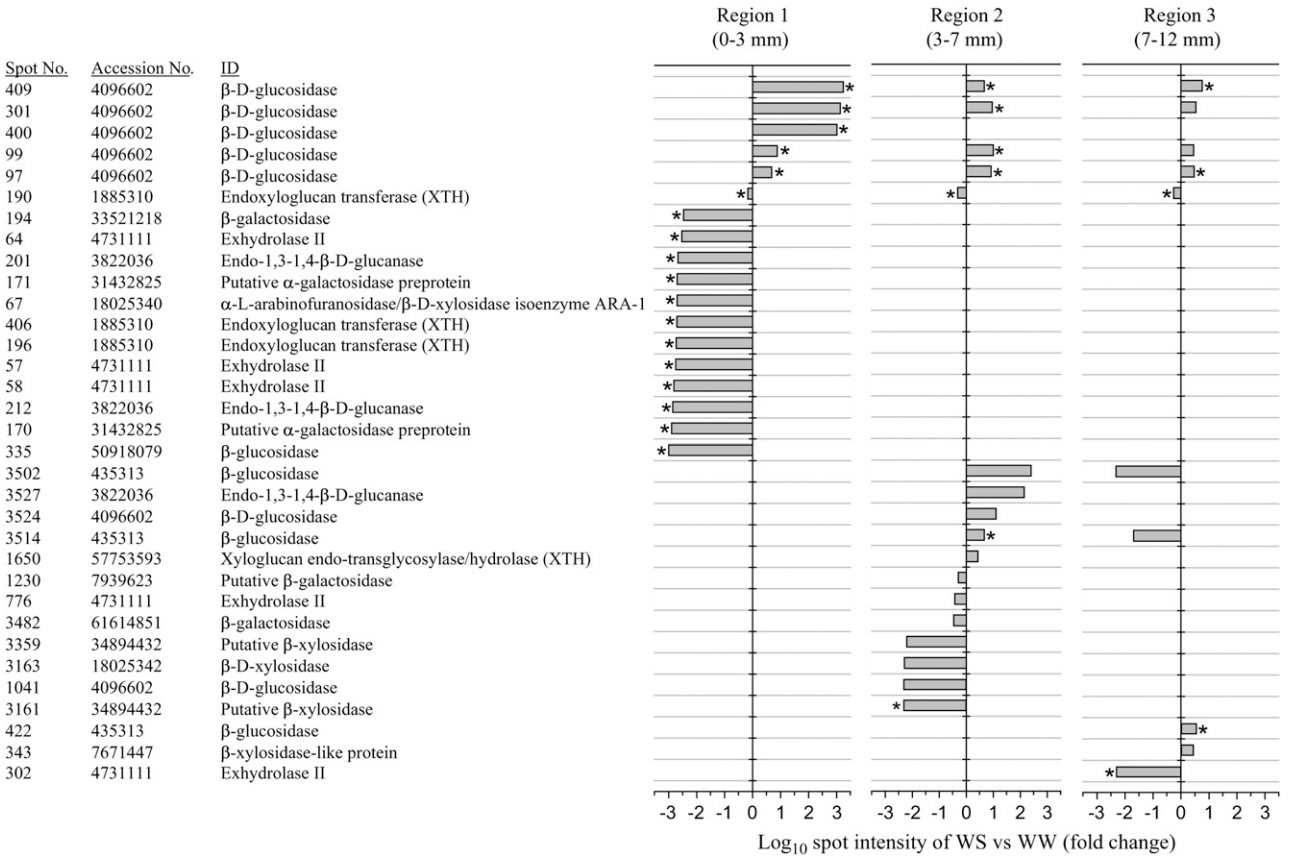

Spot No.	Accession No.	ID
409	4096602	β-D-glucosidase
301	4096602	β-D-glucosidase
400	4096602	β-D-glucosidase
99	4096602	β-D-glucosidase
97	4096602	β-D-glucosidase
190	1885310	Endoxyloglucan transferase (XTH)
194	33521218	β-galactosidase
64	4731111	Exhydrolase II
201	3822036	Endo-1,3-1,4-β-D-glucanase
171	31432825	Putative α-galactosidase preprotein
67	18025340	α-L-arabinofuranosidase/β-D-xylosidase isoenzyme ARA-1
406	1885310	Endoxyloglucan transferase (XTH)
196	1885310	Endoxyloglucan transferase (XTH)
57	4731111	Exhydrolase II
58	4731111	Exhydrolase II
212	3822036	Endo-1,3-1,4-β-D-glucanase
170	31432825	Putative α-galactosidase preprotein
335	50918079	β-glucosidase
3502	435313	β-glucosidase
3527	3822036	Endo-1,3-1,4-β-D-glucanase
3524	4096602	β-D-glucosidase
3514	435313	β-glucosidase
1650	57753593	Xyloglucan endo-transglycosylase/hydrolase (XTH)
1230	7939623	Putative β-galactosidase
776	4731111	Exhydrolase II
3482	61614851	β-galactosidase
3359	34894432	Putative β-xylosidase
3163	18025342	β-D-xylosidase
1041	4096602	β-D-glucosidase
3161	34894432	Putative β-xylosidase
422	435313	β-glucosidase
343	7671447	β-xylosidase-like protein
302	4731111	Exhydrolase II

Figure 7. Responses to water stress in R1 to R3 of fraction 1 CWPs in the category of hydrolases. See the legend of Figure 5 for full description.

compared to well-watered roots, a novel technique was developed to image apoplastic ROS levels in situ using the fluorescent indicator dye 2′,7′-dichlorodihydrofluorescein (H_2DCF; custom designed by Molecular Probes). The dye was modified in such a way that it should be impermeable to the plasma membrane (see details in ''Materials and Methods''). Confocal images of the root epidermis provided evidence of pronounced apoplastic ROS levels in R1 of water-stressed roots, whereas there was little ROS staining in the same region of well-watered roots (Fig. 12). The ROS levels in water-stressed roots were similar at several time points examined (36, 48, and 60 h after transplanting; data not shown), indicating that the increase in ROS was not a transient event. Evidence of apoplastic localization of H_2DCF staining was provided both by analysis of the pattern of staining in consecutive focal planes (Supplemental Video S1) as

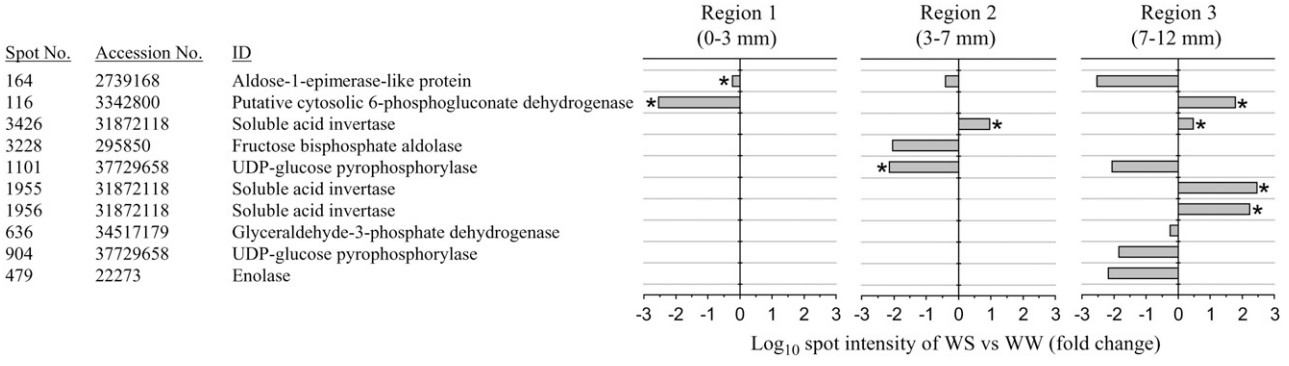

Spot No.	Accession No.	ID
164	2739168	Aldose-1-epimerase-like protein
116	3342800	Putative cytosolic 6-phosphogluconate dehydrogenase
3426	31872118	Soluble acid invertase
3228	295850	Fructose bisphosphate aldolase
1101	37729658	UDP-glucose pyrophosphorylase
1955	31872118	Soluble acid invertase
1956	31872118	Soluble acid invertase
636	34517179	Glyceraldehyde-3-phosphate dehydrogenase
904	37729658	UDP-glucose pyrophosphorylase
479	22273	Enolase

Figure 8. Responses to water stress in R1 to R3 of fraction 1 CWPs in the category of carbohydrate metabolism. See the legend of Figure 5 for full description.

Spot No.	Accession No.	ID
316	34902150	Putative r40c1 protein
168	34588146	α-1,4-glucan-protein synthase
365	13194668	Unknown
155	34912572	Putative integral membrane Yip1 family protein
98	50511452	Putative β-N-acetylhexosaminidase
3337	55297457	Putative lipase
3464	28950668	Legumin-like protein
3507	28950668	Legumin-like protein
3385	34894958	Putative lipoamide dehydrogenase
920	52076641	Putative PS60
688	4582787	Adenosine kinase
1518	21206625	Putative leucine aminopeptidase
1948	50925937	OSJNBb0091E11.17
1902	55297457	Putative lipase
1434	50915542	Cytochrome b5 domain-containing protein-like
855	55297457	Putative lipase
1334	11493677	Profilin 5
604	50943229	Putative 41 kD chloroplast nucleoid DNA binding protein
959	42571485	Oxidoreductase NAD-binding domain-containing protein
1158	50725506	Putative ubiquitin-conjugating enzyme family protein
1020	23955914	Translationally controlled tumor protein-like protein

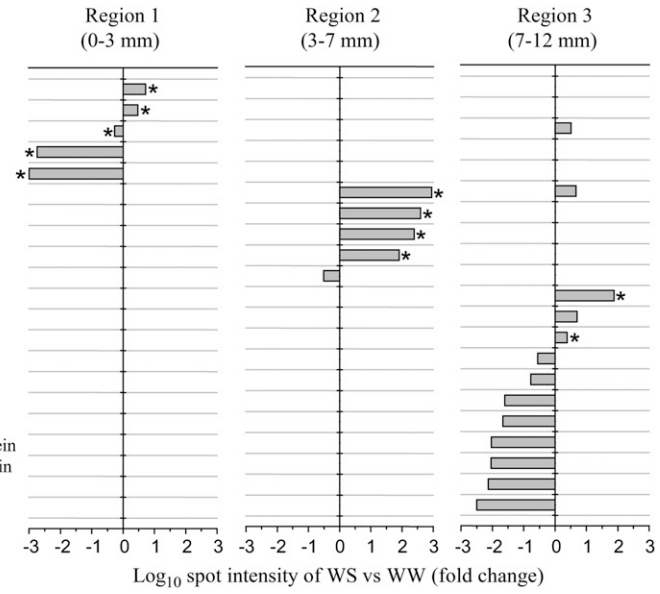

Figure 9. Responses to water stress in R1 to R3 of fraction 1 CWPs in the category of other/unknown. See the legend of Figure 5 for full description.

well as by comparison to the different staining pattern obtained using 5-(and-6)-carboxy-2′,7′-H_2DCF diacetate (carboxy-H_2DCFDA), an unmodified dye that is permeable to the membrane. The membrane-permeable dye showed distinct staining of the cytoplasm and cellular organelles (Fig. 12, inset), whereas there was no evidence of intracellular staining using H_2DCF. It should be noted that in contrast to the root epidermal cells, detached and mature root cap cells showed obvious cytoplasmic and nuclear staining with H_2DCF (Fig. 12), probably due to impairment of plasma membrane integrity associated with the onset of apoptosis. The distinct staining pattern of the root cap cells further reinforces the conclusion that H_2DCF staining of the root epidermal cells in R1 was restricted within the apoplast.

Efforts were also made to analyze apoplastic ROS levels in R2 using H_2DCF staining. However, the results suggested that the use of the dye in R2 was unreliable. There was often evidence of cytosolic staining in both the well-watered and water-stressed roots, indicating some degree of membrane permeability to the dye in the epidermal cells of this region. Thus, these results are not presented.

DISCUSSION

Identification and Spatial Distribution of Fraction 1 CWPs in the Root Elongation Zone

Using validated methods for fraction 1 CWP extraction from the maize primary root elongation zone (Zhu et al., 2006) in combination with mass spectrometry analysis, a total of 152 proteins were identified from water stress-responsive protein spots on 2-DE gels from three regions that exhibited distinct responses of elongation rate to water stress. In agreement with the findings of our previous study (Zhu et al., 2006), in which the analysis was limited to the whole elongation zone of well-watered roots with no spatial resolution, the results indicate that the method effectively enriched for CWPs with minimal cytosolic contamination. First, a large number of the proteins identified in this study have also been isolated from cell walls using other approaches, and many of these proteins are related to cell wall metabolism and structural modification (Fry, 1988). Second, 105 of the 152 proteins (69%) have an N-terminal signal peptide, whereas it was previously shown that only 3% of proteins identified in an extract of total soluble proteins from the root elongation zone have signal peptides (Zhu et al., 2006). In addition, increasing evidence suggests that proteins can be secreted into cell walls without having a signal peptide (Voigt and Frank, 2003; Slabas et al., 2004; Juarez-Diaz et al., 2006). Consistent with this model, 17 of the proteins were predicted to be so-called nonclassical secretory proteins (Bendtsen et al., 2004; Zhu et al., 2006), and among the 30 remaining proteins, 19 were previously identified in cell walls including two malate dehydrogenases, two glyoxalases I, three UDP-Glc pyrophosphorylases, and 12 β-D-glucosidases (Gross, 1977; Fry, 1988; Li et al., 1989; Chivasa et al., 2002; Pitarch et al., 2002; Kleczkowski et al., 2004; Watson et al., 2004).

Among the 152 identified proteins, 61 (40%) were not identified in our previous study of the cell wall proteome from the elongation zone of well-watered roots (Zhu et al., 2006). The presence of many newly identified proteins was due partly to the imposition of water stress that increased the abundance of particular

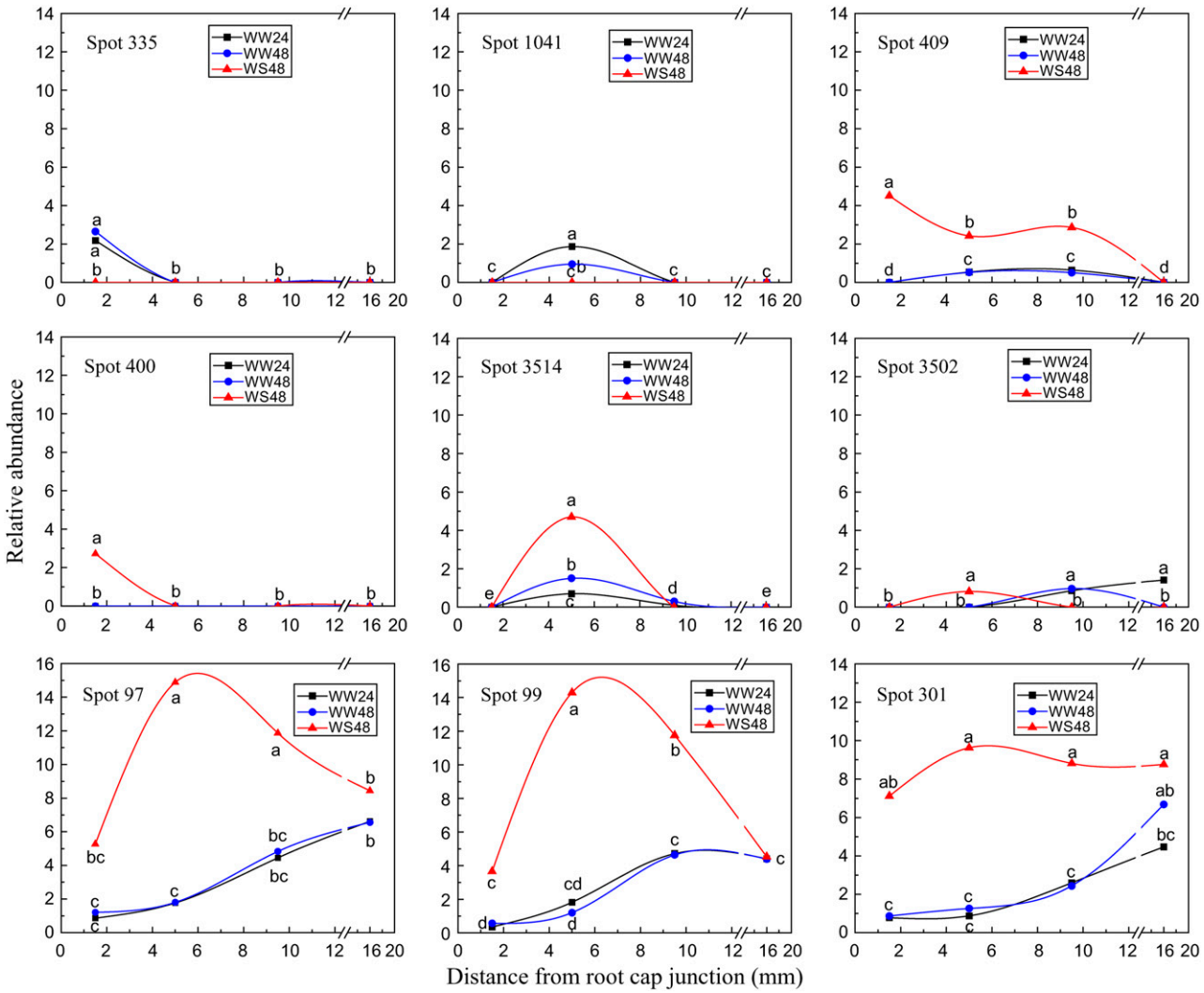

Figure 10. Spatial distribution of protein abundance for nine β-D-glucosidases in R1 to R4 of roots grown under well-watered (WW24 [developmental control] and WW48 [temporal control]) or water-stressed (WS48) conditions. The fitted lines were smoothed using the SPLINE method. Different letters indicate significant differences at the $P < 0.05$ level.

proteins, and partly to the spatial profiling that may have resulted in an enrichment of proteins in specific regions of the elongation zone.

The spatial distributions of protein abundance in relation to the elongation rate profiles provide insight into potential functions for some of the proteins (Fig. 10; Supplemental Figs. S1–S5). This spatial resolution also helps to distinguish the function of different proteins in the same family. As shown in Figure 10, nine spots that were identified as β-D-glucosidase showed widely varying spatial profiles in well-watered roots, implying that the proteins may have different roles associated with specific processes in the different regions. The differential responses of these proteins to water stress further support the notion that these proteins function differently. Another example of significant variation both in abundance profiles and in the pattern of response to water stress between proteins in the same family is provided by the peroxidases (Supplemental Fig. S1). Potential functions of β-D-glucosidases and peroxidases are discussed further in the following sections.

It should be noted that the R1 samples included the root cap in addition to the apical 3 mm of the root (additional washing steps were included to remove the majority of border cells from the root cap periphery). Thus, a fraction of the proteins identified in R1 may be extracellular proteins derived from the root cap. A comparison was made with a recent report on the pea (*Pisum sativum*) root cap secretome (Wen et al., 2007), which revealed that only four of the root cap proteins matched with the 53 proteins identified in R1. These results suggest that the contribution of proteins secreted from the root cap was minor.

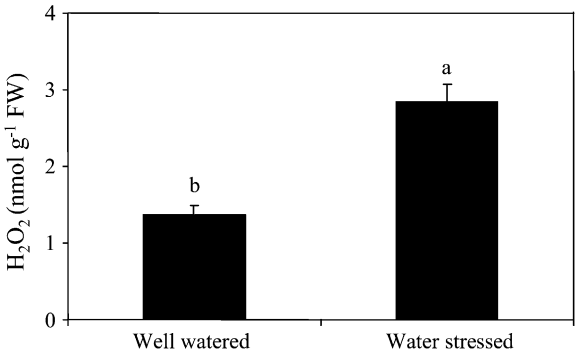

Figure 11. Apoplastic H_2O_2 content in R1 of roots grown under well-watered or water-stressed conditions for 48 h after transplanting. Data are means ± SE ($n = 3$). Different letters indicate significant difference at the $P < 0.01$ level. FW, Fresh weight.

Increased Apoplastic ROS in Water-Stressed Roots—Potential Role in Enhanced Cell Wall Loosening

One large group of CWPs that showed changes in abundance under water stress are related to ROS metabolism (Fig. 5). ROS, including superoxide radicals, H_2O_2, and hydroxyl radicals, are normally produced in various cell compartments including the apoplast (Mittler et al., 2004). Increased ROS production often occurs under abiotic and biotic stress conditions, including water deficit, and can be associated with oxidative damage (Iturbe-Ormaetxe et al., 1998). Thus, it is possible that the changes in proteins associated with ROS metabolism may play a role in scavenging ROS and thereby preventing oxidative damage to the root cell walls and plasma membrane under water stress conditions (Apel and Hirt, 2004). However, it is notable that in R1, the six proteins in this category that increased in abundance included two putative oxalate oxidase/germin proteins and a superoxide dismutase, which contribute to H_2O_2 production (Lane, 1994; Pignocchi and Foyer, 2003), and two peroxidases/peroxidase precursors, which can also contribute to ROS production including the generation of hydroxyl radicals from H_2O_2 (Schweikert et al., 2000; Liszkay et al., 2003; Passardi et al., 2004). Thus, these changes in protein abundance suggested that apoplastic ROS levels may have increased in R1 of the water-stressed roots. This hypothesis was tested and confirmed both by quantification of H_2O_2 content in extracted apoplastic fluid and by in situ imaging of apoplastic ROS (Figs. 11 and 12).

The increase in apoplastic ROS in R1 under water deficit conditions could be involved in the enhanced longitudinal extensibility of the cell walls in this region of water-stressed compared to well-watered roots (Wu et al., 1996) and, thereby, in the maintenance of cell elongation despite reduced turgor pressure (Spollen and Sharp, 1991). Recent studies suggest that generation of hydroxyl radicals from H_2O_2 (by either the Fenton reaction or peroxidase activity) can play a direct role in cell wall loosening via polysaccharide cleavage (Fry, 1998; Fry et al., 2001; Liszkay et al., 2003), and there is evidence for this activity in the elongation zone of leaves (Rodriguez et al., 2002) and primary roots (Liszkay et al., 2004) of well-watered maize. Further, there is evidence that salinity-induced inhibition of leaf expansion in maize is associated with reduced apoplastic ROS production (Rodriguez et al., 2004, 2007). However, to our knowledge, up-regulation of this mechanism of wall loosening in the response of root growth to water stress has not been investigated. Indeed, enhanced cell wall loosening as an adaptive response to stress conditions has been little studied, being limited to investigations of the maintenance of elongation in water-stressed roots (for review, see

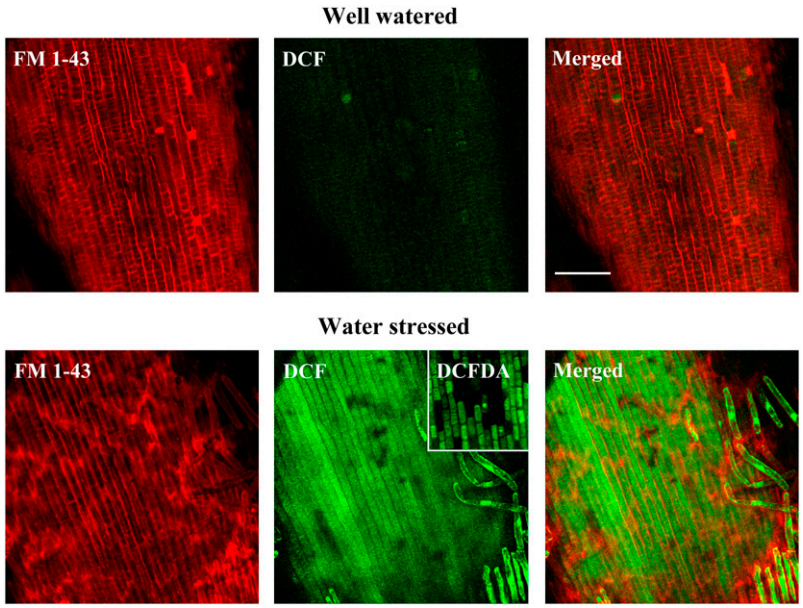

Figure 12. Representative images of apoplastic ROS as indicated by staining with H_2DCF (DCF, green fluorescence), a custom designed membrane-impermeable ROS indicator, in the epidermis of R1 (approximately 1.5 mm from the apex) of roots grown under well-watered (top sections) or water-stressed (bottom sections) conditions for 48 h after transplanting. The roots were also stained with the membrane probe FM 1-43 (red fluorescence) to visualize the cellular structure. The images are composed of projections of 13 optical section planes (3 μm in thickness) obtained by a two-photon laser-scanning confocal microscope. In contrast to the apoplastic localization of ROS staining with H_2DCF in the root epidermis, several detached and mature root cap cells showed cytoplasmic and nuclear staining with H_2DCF. The inset image is from R1 of a water-stressed root stained for cytosolic ROS with carboxy-H_2DCFDA (DCFDA), a membrane-permeable ROS indicator. Scale bar represents 100 μm and applies for all images. See Supplemental Video S1 for additional detail.

Spollen et al., 1993; Pritchard, 1994; Wu and Cosgrove, 2000) and the stimulation of stem elongation in submerged deepwater rice (*Oryza sativa*) and other plants (Cho and Kende, 1997; Vreeburg et al., 2005). Our findings suggest that increased apoplastic ROS production may play a positive rather than a negative role in regulating the root growth response under severe water stress.

ROS have also been proposed to act as signaling molecules in various processes (e.g. Moller et al., 2007). We found that the increase in apoplastic ROS level in R1 of water-stressed compared to well-watered roots was similar at all the time points examined (36, 48, and 60 h after water stress imposition). Thus, it seems likely that the increase in ROS was related to a continuing process of stress adaptation rather than a transient signaling event during stress development.

In contrast to the possible role of peroxidases in ROS production and cell wall loosening in R1, the abundance of two peroxidases also increased in R3 of water-stressed compared to well-watered roots, while that of several others decreased. Since elongation ceased in R3 under water stress, these peroxidases may be involved in other processes including cell wall stiffening by oxidative cross-linking of wall phenolics (Fry, 1988).

Other Water Stress-Responsive Proteins and Their Potential Functions

Most of the identified proteins in the defense and detoxification category are known to be involved in pathogenesis and insect defense, including polygalacturonase inhibitor proteins, chitinases, and nodulin precursors. In general, these proteins decreased in abundance throughout the elongation zone in water-stressed compared to well-watered roots. This could represent a mechanism to redirect resources and energy for abiotic stress adaptation. However, a few proteins in this category, including two polygalacturonase inhibitor proteins in R1 and an osmotin in R3, increased in abundance under water stress. These particular proteins may be important in the general defense responses of stressed plants. Osmotin, for example, was shown to be involved in responses to NaCl, desiccation, ethylene, abscisic acid (ABA), and UV treatments as well as in resistance to fungal and viral attack (Liu et al., 1994).

The largest group of water stress-responsive CWPs identified in this study was the category of hydrolases (Fig. 7). In R1, the abundance of most hydrolases decreased markedly in the water-stressed roots. It was previously shown that the deposition rate and content of cell wall mass per unit length of root was decreased in the elongation zone of water-stressed compared to well-watered maize primary roots (Wu et al., 1994). Therefore, an overall reduction in cell wall hydrolases may reflect lower cell wall polysaccharide metabolism in water-stressed roots. However, three XTHs and two endo-1,3;1,4-β-D-glucanases, which are endocleavage type hydrolases and implicated in cell wall loosening processes (Nishitani and Tominaga, 1991; Fry et al., 1992; Kim et al., 2000), also decreased in abundance in R1 of the water-stressed roots. The decreased abundance of the XTHs, in particular, was unexpected since a previous study using the same experimental system (although with a different genotype) showed that the total extractable xyloglucan endotransglucosylase activity (XET; one of the two known activities of XTH proteins; Rose et al., 2002) was greater in R1 and R2 of water-stressed compared to well-watered roots (Wu et al., 1994), suggesting that XTH may be involved in the stress-induced enhancement of cell wall extensibility in the apical region. Moreover, the abundance profiles of these XTHs showed a close correlation with the spatial distribution of elongation rate in the well-watered roots (Supplemental Fig. S3). One of the possible explanations for the discrepancy between the XET activity and XTH protein abundance is that the XET activity was assayed from total soluble protein extracts and may not represent the activity of XTH specifically in the cell walls. It is also possible that XET activity was regulated at the posttranslational level. Thus, subtle protein modifications, which were not detected in this study, might lead to increased XET activity in water-stressed roots despite a decrease in protein abundance.

Interestingly, the only proteins in the hydrolase category that increased in abundance in R1 of the water-stressed roots were a group of five β-D-glucosidases (Figs. 7 and 10). Although exocleavage-type hydrolases are implicated in regulating cell elongation (Huber and Nevins, 1981; Kim et al., 2000), the β-D-glucosidases identified in this study may not play the same role since most of these proteins also increased in abundance in R2 and R3 under water stress where cell elongation had slowed or ceased, respectively (Fig. 1). There is evidence that β-D-glucosidase activity in the root apoplast functions in releasing free ABA from the ABA conjugate ABA-Glc ester, which may serve as a long-distance transport form (Hartung et al., 2002; Sauter et al., 2002; Lee et al., 2006; Schroeder and Nambara, 2006). ABA accumulates to high concentrations in the root elongation zone under water-stressed conditions, particularly toward the apex (Saab et al., 1992), and the accumulation is required for the maintenance of root elongation (Saab et al., 1990; Sharp et al., 1994; Sharp, 2002). Accordingly, the stress-induced increase in abundance of several β-D-glucosidases may be involved in ABA release from conjugated ABA transported to the elongation zone.

Apoplastic β-D-glucosidases have also been implicated in lignin synthesis. One of the proposed mechanisms for lignin synthesis is that monolignols are synthesized inside the cell and secreted into the cell wall as monolignol glucosides, where β-D-glucosidases hydrolyze the glucoside and release monolignols for lignin synthesis (Whetten et al., 1998). In this case, the β-D-glucosidases may play roles in reducing cell wall extensibility and inhibiting cell elongation in R2 and

R3 of the water-stressed roots. Consistent with this possibility, Fan et al. (2006) published evidence for increased lignin metabolism in association with reduced cell wall extensibility in the basal region of the elongation zone in water-stressed maize primary roots.

Among the carbohydrate metabolism-related CWPs, three acid invertases increased in abundance in R2 and R3 of the water-stressed roots (Fig. 8). Interestingly, Tang et al. (1999) reported that antisense repression of a cell wall invertase resulted in a drastic decrease in taproot growth and development in carrot (*Daucus carota*). The smaller taproots were associated with a lower level of carbohydrate in roots but an elevated level of Suc and starch in leaves, suggesting that cell wall invertase plays an important role in Suc partitioning. In maize seedlings, primary root growth is dependent on the Suc supply from the kernel, and in particular, water-stressed roots accumulate a significant amount of sugars for osmotic adjustment in the elongation zone (Sharp et al., 1990). Thus, an increase in cell wall invertase (and activity) could create a strong sink to enhance Suc transport from the kernel to the roots to maintain a supply of sugars for root growth and stress adaptation.

The CWPs in the category of other/unknown further reflect the complexity of the response to water stress (Fig. 9). There are indications of regulation of protein modification involving α-1,4-glucan protein synthase, carbohydrate modification involving putative β-*N*-acetylhexosaminidase, and lipid modification, presumably associated with the plasma membrane, involving lipases. The involvement of many other proteins in the stress response remains unknown. For example, two legumin-like proteins were up-regulated specifically in R2. Legumin-like proteins are seed storage proteins and are usually found in seed endosperm (Meakin and Gatehouse, 1991). It is not clear whether these proteins perform a similar role for nutrient storage in the root elongation zone or whether they perform different roles. Further work is necessary to address the functionality of these proteins.

CONCLUSION

The results reveal major and predominantly region-specific changes in fraction 1 CWP composition in the elongation zone of water-stressed compared to well-watered roots. Stress-induced changes in CWPs are involved in multiple processes that regulate the pattern of response of cell elongation within the elongation zone. In particular, the protein identifications predicted that apoplastic ROS levels are increased in the apical region of the elongation zone in water-stressed roots, which was confirmed by quantification of H_2O_2 and in situ imaging. This response could contribute directly to the known enhancement of wall loosening in this region and, thereby, the maintenance of cell elongation despite reduced turgor pressure. Future studies of the tightly ionically bound and covalently bound CWP fractions will provide additional insight into the complexity of mechanisms that regulate root growth under water stress.

MATERIALS AND METHODS

Maize Seedling Culture, Harvest, and Extraction of Water Soluble Plus Lightly Ionically Bound CWPs

Maize (*Zea mays* 'FR697') seeds were surface sterilized in 0.3% NaOCl solution for 15 min, rinsed with distilled water, and imbibed for 24 h in aerated 1 mM $CaSO_4$. The seeds were germinated in vermiculite (no. 2A, Therm-O-Rock East Inc.), which was well moistened with 1 mM $CaSO_4$, for 28 h at 29°C and near-saturation humidity in the dark (Spollen et al., 2000). Seedlings with primary roots approximately 10 mm in length were transplanted to plastic containers containing vermiculite at water potentials of −0.03 MPa (well watered) or −1.6 MPa (water stressed), which were obtained by thorough mixing with different amounts of 1 mM $CaSO_4$. Vermiculite water potentials were measured by isopiestic thermocouple psychrometry (Boyer and Knipling, 1965). The seedlings were then grown under the same conditions until the primary roots were harvested at 24 h (developmental control, roots of the same length as the water stressed treatment) and 48 h (temporal control, roots of the same age as the water-stressed treatment) after transplanting in the well-watered treatment, and at 48 h after transplanting in the water-stressed treatment. The apical 20 mm of each root was sectioned into four regions (distances are from the root cap junction): R1, 0 to 3 mm plus the root cap; R2, 3 to 7 mm; R3, 7 to 12 mm; R4, 12 to 20 mm. Transplanting and harvesting were performed using a green safelight (Saab et al., 1990).

Immediately after harvest, the root segments were transferred into 20 mM ice-cold K_2HPO_4 solution (pH 6.0). The segments were then rinsed twice with distilled, deionized water and twice with 0.01 M MES buffer; it should be noted that these steps probably removed the majority of border cells from the root cap periphery (Wen et al., 2007). Water soluble and lightly ionically bound CWPs were then extracted according to the method optimized for the maize primary root elongation zone by Zhu et al. (2006). At each harvest of each treatment, three batches of 50 segments per region were used for CWP extraction; the extracts from the three batches were combined to produce a subsample. Five subsamples were pooled for each of three replicate samples per region for each treatment (i.e. CWPs were extracted from a total of 750 segments per sample).

Protein Separation by 2-DE

Prior to 2-DE, the CWP samples were precipitated overnight at −70°C with 10% (w/v) TCA, and the pellets were washed three times with ice-cold methanol and dried briefly. The proteins were quantified using either Bio-Rad RCDC Protein Microassay (Bio-Rad) or RediPlate EZQ Protein Quantitation kit (Molecular Probes) according to the manufacturer's recommendations. Samples of 7 μg protein were solubilized in 185 μL of an isoelectric focusing buffer (Sequential Extraction buffer 3; Bio-Rad). 2-DE was carried out as previously described (Zhu et al., 2006). After electrophoresis, gels were fixed in 7% acetic acid, 10% methanol for 1 h, and stained overnight with SyproRuby (Molecular Probes). The stained gels were washed in 7% acetic acid, 10% methanol for 1 h, and rinsed with water.

Image Analysis of 2-DE Gels

Protein spots were visualized using the TYPHOON 9410 system (Amersham Biosciences). Gels containing the three replicate samples from each treatment and each region were analyzed with Phoretix 2D Evolution software (Nonlinear Dynamics) enabling spot detection, quantification, and spot matching across different gels. The automatic spot detection and matching was followed by a manual correction. Experimental M_rs were calibrated using commercial molecular mass standards run in a separate marker lane on the 2-DE gels, and the experimental pIs were calibrated according to Bio-Rad IPG strip specifications.

After subtracting background with the nonspot mode (margin 45), spot volumes were normalized by dividing each spot volume by the total volume of all spots present in all gels. The normalized spot volumes were used to determine the quantitative variation of protein expression across the treatments

and regions. Region-specific water deficit-responsive spots were identified after normalizations within the batch of nine gel images (three replicates for each of three treatments) from each region. All 36 gel images were normalized for across-region comparisons of protein abundance. To determine the statistical significance of changes in protein abundance, a multiple comparison of means (Student-Newman-Keuls test) was performed with normalized protein spot volume as variables and control or treatment as factors, and a confidence level of 95% (SAS 5.1, SAS Institute Inc.). For proteins that were not detected in one condition when compared to another, a protein abundance of 0.001, which was the minimal value of spot intensity, was used for calculation of fold-change.

Protein Identification by HPLC-Electrospray Quadrupole Time-of-Flight Mass Spectrometry

Proteins differentially expressed were excised from gels and digested as described in Zhu et al. (2006). Peptide separation was performed by nanoflow HPLC (Ultimate). Five microliters of protein digests were loaded onto a C18 precolumn (LC Packing) for desalting and concentrating. Peptides were then eluted from the precolumn and separated on a nanoflow analytical C18 column and analyzed using an ABI QSTAR XL (Applied Biosystems/MDS Sciex) as described in Zhu et al. (2006). Time-of-flight mass spectrometry spectra and product ion spectra were acquired using Analyst QS software. The peptide tandem mass spectra were searched against the maizeseq.org MAIZE EST database (www.maizeseq.org) using MASCOT search engine (http://www.matrixscience.com). Unambiguous identification was judged by the number of peptide sequence tags, sequence coverage, mowse score, the quality of tandem mass spectrometry spectra, and reproducibility of identification across gels.

Apoplastic H_2O_2 Assay

Apoplastic fluid from R1 of roots grown under well-watered or water-stressed conditions for 48 h was extracted by the vacuum infiltration and centrifugation method described in Zhu et al. (2006) except without the desalting procedure. The H_2O_2 content was quantified using an Amplex Red Hydrogen Peroxide/Peroxidase Assay kit (Molecular Probes).

In Situ Imaging of Apoplastic ROS

A novel dye, H_2DCF, was custom synthesized for this study (Molecular Probes). The dye is a derivative of carboxy-H_2DCFDA, which is a fluorescent indicator of intracellular ROS (Maxwell et al., 1999), in which the acetate groups (which allow the molecule to cross the plasma membrane) have been cleaved. Therefore, H_2DCF should be restricted within the cell wall and apoplastic space.

Seedlings were grown in vermiculite under either well-watered or water-stressed conditions as described above. At 36, 48, or 60 h after transplanting, the seedlings were removed from the vermiculite and the tips of intact primary roots were immersed in a staining agarose solution. The solution was prepared as a combination of 1% high- and 1% low-gelling temperature agarose (1:1) in 1 mM $CaSO_4$, which solidified at approximately 30°C. The solution was allowed to cool and as it approached 30°C, H_2DCF and the fluorescent membrane probe FM 1-43 [*N*-(3-triethylammoniumpropyl)-4-(4-(dibutylamino) styryl) pyridinium dibromide; Molecular Probes] were added at final concentrations of 30 μM and 50 μg/mL, respectively. Roots were then immersed immediately before the onset of solidification. For the staining of water-stressed roots, the water potential of the agarose solution was adjusted to −1.6 MPa (the same water potential as the vermiculite in which the roots were growing) by addition of melibiose to avoid imposing an osmotic shock to the roots. Melibiose was chosen for this purpose because of evidence that it is neither hydrolyzed nor taken up by cells (Dracup et al., 1986). The agarose staining solution was developed to minimize potential diffusion of H_2DCF and ROS from the apoplast after immersion of the roots. After 30 min of staining, when the agarose had solidified, an agarose block containing the apical 20 mm of the root was removed and placed on a cover glass for confocal imaging; thus, the root tip was not mechanically disturbed. Since the confocal laser could penetrate through the agarose, the agarose around the root did not affect the imaging process. In some experiments, water-stressed roots were stained using the same procedures but with 15 μM carboxy-H_2DCFDA (Molecular Probes) for imaging of intracellular ROS.

The epidermal cells were imaged for H_2DCF fluorescence using two-photon laser-scanning confocal microscopy (Zeiss LSM NLO 510 combined with a Coherent, Chameleon 720–950 nm tunable two photon laser) at 750 nm infrared excitation wavelength, and the emission was captured between 500 to 550 nm. The images were scanned without scan averaging (fast acquisition) using a 10× (EC Plan-NeoFluar NA 0.3) objective together with 1.9 digital zoom under 512 pixel resolution in XY. The power, gain, offset, and detector gain levels were optimized and kept constant between different experimental samples in a given day. FM 1-43 and carboxy-H_2DCFDA imaging processes were the same as for H_2DCF with the exception of excitation and emission wavelengths, which were 543 nm and 565 to 615 nm, and 488 nm and 500 to 550 nm, respectively. All images were processed by LSM 5 Image Examiner under identical conditions.

Supplemental Data

The following materials are available in the online version of this article.

Supplemental Figure S1. Spatial distribution of abundance for CWPs in the category of ROS metabolism.

Supplemental Figure S2. Spatial distribution of abundance for CWPs in the category of defense and detoxification.

Supplemental Figure S3. Spatial distribution of abundance for CWPs in the category of hydrolases.

Supplemental Figure S4. Spatial distribution of abundance for CWPs in the category of carbohydrate metabolism.

Supplemental Figure S5. Spatial distribution of abundance for CWPs in the category of other/unknown.

Supplemental Table S1. Identities of water deficit-responsive protein spots from the 2-DE gels of water soluble and lightly ionically bound (fraction 1) CWPs.

Supplemental Video S1. Consecutive focal planes of the merged confocal image of a water-stressed root presented in Figure 12.

ACKNOWLEDGMENTS

We thank Dr. Georgia Davis (University of Missouri, Columbia) for providing seed of maize 'FR697', and Drs. William Spollen, Jay Thelen, and Brian Mooney (University of Missouri, Columbia) for helpful consultation. We also thank Dr. Steve Schroeder (University of Missouri, Columbia) and Johann Joets and Olivier Langella (Unité Mixte de Recherche de Genetique Vegetale du Moulon, Institut National de la Recherche Agronomique/Centre National de la Recherche Scientifique/Universitat Paris XI/Institute National Agronomique Paris-Grignon, Gif sur Yvette, France) for help in building the modified PROTICdb and making the data publicly accessible.

Received August 11, 2007; accepted October 13, 2007; published October 19, 2007.

LITERATURE CITED

Apel K, Hirt H (2004) Reactive oxygen species: metabolism, oxidative stress, and signal transduction. Annu Rev Plant Biol **55:** 373–399

Bayer EM, Bottrill AR, Walshaw J, Vigouroux M, Naldrett MJ, Thomas CL, Maule AJ (2006) Arabidopsis cell wall proteome defined using multidimensional protein identification technology. Proteomics **6:** 301–311

Bendtsen JD, Jensen LJ, Blom N, von Heijne G, Brunak S (2004) Feature-based prediction of non-classical and leaderless protein secretion. Protein Eng Des Sel **17:** 349–356

Blee KA, Wheatley ER, Bonham VA, Mitchell GP, Robertson D, Slabas AR, Burrell MM, Wojtaszek P, Bolwell GP (2001) Proteomic analysis reveals a novel set of cell wall proteins in a transformed tobacco cell culture that synthesises secondary walls as determined by biochemical and morphological parameters. Planta **212:** 404–415

Boudart G, Jamet E, Rossignol M, Lafitte C, Borderies G, Jauneau A, Esquerre-Tugaye MT, Pont-Lezica R (2005) Cell wall proteins in apo-

plastic fluids of *Arabidopsis thaliana* rosettes: identification by mass spectrometry and bioinformatics. Proteomics **5:** 212–221

Boyer JS, Knipling EB (1965) Isopiestic technique for measuring leaf water potentials with a thermocouple psychrometer. Proc Natl Acad Sci USA **54:** 1044–1051

Chivasa S, Ndimba BK, Simon WJ, Robertson D, Yu XL, Knox JP, Bolwell P, Slabas AR (2002) Proteomic analysis of the *Arabidopsis thaliana* cell wall. Electrophoresis **23:** 1754–1765

Cho HT, Kende H (1997) Expansins and internodal growth of deepwater rice. Plant Physiol **113:** 1145–1151

Dani V, Simon WJ, Duranti M, Croy RRD (2005) Changes in the tobacco leaf apoplast proteome in response to salt stress. Proteomics **5:** 737–745

Dracup M, Gibbs J, Greenway H (1986) Melibiose, a suitable, non-permeating osmoticum for suspension-cultured tobacco cells. J Exp Bot **37:** 1079–1089

Fan L, Linker R, Gepstein S, Tanimoto E, Yamamoto R, Neumann PM (2006) Progressive inhibition by water deficit of cell wall extensibility and growth along the elongation zone of maize roots is related to increased lignin metabolism and progressive stelar accumulation of wall phenolics. Plant Physiol **140:** 603–612

Fan L, Neumann PM (2004) The spatially variable inhibition by water deficit of maize root growth correlates with altered profiles of proton flux and cell wall pH. Plant Physiol **135:** 2291–2300

Ferry-Dumazet H, Houel G, Montalent P, Moreau L, Langella O, Negroni L, Vincent D, Lalanne C, de Daruvar A, Plomion C, et al (2005) PROTICdb: a web-based application to store, track, query, and compare plant proteome data. Proteomics **5:** 2069–2081

Fry SC (1988) The Growing Plant Cell Wall: Chemical and Metabolic Analysis. Longman Scientific & Technical, Harlow, UK

Fry SC (1998) Oxidative scission of plant cell wall polysaccharides by ascorbate-induced hydroxyl radicals. Biochem J **332:** 507–515

Fry SC, Dumville JC, Miller JG (2001) Fingerprinting of polysaccharides attacked by hydroxyl radicals in vitro and in the cell walls of ripening pear fruit. Biochem J **357:** 729–737

Fry SC, Smith RC, Renwick KF, Martin DJ, Hodge SK, Matthews KJ (1992) Xyloglucan endotransglycosylase, a new wall-loosening enzyme activity from plants. Biochem J **282:** 821–828

Gross GG (1977) Cell wall-bound malate dehydrogenase from horseradish. Phytochemistry **16:** 319–321

Hartung W, Sauter A, Hose E (2002) Abscisic acid in the xylem: where does it come from, where does it go to? J Exp Bot **366:** 27–32

Haslam RP, Downie AL, Raveton M, Gallardo K, Job D, Pallett KE, John P, Parry MAJ, Coleman JOD (2003) The assessment of enriched apoplastic extracts using proteomic approaches. Ann Appl Biol **143:** 81–91

Huber DJ, Nevins DJ (1981) Partial purification of endo- and exo-β-glucanase enzymes from *Zea mays* L. seedlings and their involvement in cell-wall autohydrolysis. Planta **151:** 206–214

Iturbe-Ormaetxe I, Escuredo PR, Arrese-Igor C, Becana M (1998) Oxidative damage in pea plants exposed to water deficit or paraquat. Plant Physiol **116:** 173–181

Juarez-Diaz JA, McClure B, Vazquez-Santana S, Guevara-Garcia A, Leon-Mejia P, Marquez-Guzman J, Cruz-Garcia F (2006) A novel thioredoxin *h* is secreted in *Nicotiana alata* and reduces S-RNase *in vitro*. J Biol Chem **281:** 3418–3424

Kim JB, Olek AT, Carpita NC (2000) Cell wall and membrane-associated exo-β-glucanases from developing maize seedlings. Plant Physiol **123:** 471–486

Kleczkowski LA, Geisler M, Ciereszko I, Johansson H (2004) UDP-glucose pyrophosphorylase: an old protein with new tricks. Plant Physiol **134:** 912–918

Lane BG (1994) Oxalate, germin, and the extracellular matrix of higher plants. FASEB J **8:** 294–301

Lee KH, Piao HL, Kim HY, Choi SM, Jiang F, Hartung W, Hwang I, Kwak JM, Lee IJ, Hwang I (2006) Activation of glucosidase via stress-induced polymerization rapidly increases active pools of abscisic acid. Cell **126:** 1109–1120

Li ZC, McClure JW, Hagerman AE (1989) Soluble and bound apoplastic activity for peroxidase, β-D-glucosidase, malate dehydrogenase, and nonspecific arylesterase, in barley (*Hordeum vulgare* L.) and oat (*Avena sativa* L.) primary leaves. Plant Physiol **90:** 185–190

Liang BM, Sharp RE, Baskin TI (1997) Regulation of growth anisotropy in well-watered and water-stressed maize roots. I. Spatial distribution of longitudinal, radial, and tangential expansion rates. Plant Physiol **115:** 101–111

Liszkay A, Kenk B, Schopfer P (2003) Evidence for the involvement of cell wall peroxidase in the generation of hydroxyl radicals mediating extension growth. Planta **217:** 658–667

Liszkay A, van der Zalm E, Schopfer P (2004) Production of reactive oxygen intermediates (O_2^-, H_2O_2, and OH) by maize roots and their role in wall loosening and elongation growth. Plant Physiol **136:** 3114–3123

Liu D, Raghothama KG, Hasegawa PM, Bressan RA (1994) Osmotin overexpression in potato delays development of disease symptoms. Proc Natl Acad Sci USA **91:** 1888–1892

Maxwell DP, Wang Y, McIntosh L (1999) The alternative oxidase lowers mitochondrial reactive oxygen production in plant cells. Proc Natl Acad Sci USA **96:** 8271–8276

McQueen-Mason S, Durachko DM, Cosgrove DJ (1992) Two endogenous proteins that induce cell wall extension in plants. Plant Cell **4:** 1425–1433

Meakin PJ, Gatehouse JA (1991) Interaction of seed nuclear proteins with transcriptionally-enhancing regions of the pea (*Pisum sativum* L.) *legA* gene promoter. Planta **183:** 471–477

Mittler R, Vanderauwera S, Gollery M, Van Breusegem F (2004) Reactive oxygen gene network of plants. Trends Plant Sci **9:** 490–498

Moller IM, Jensen PE, Hansson A (2007) Oxidative modifications to cellular components in plants. Annu Rev Plant Biol **58:** 459–481

Nielsen H, Engelbrecht J, Brunak S, von Heijne G (1997) Identification of prokaryotic and eukaryotic signal peptides and prediction of their cleavage sites. Protein Eng **10:** 1–6

Nishitani K, Tominaga R (1991) In vitro molecular weight increase in xyloglucans by an apoplastic enzyme preparation from epicotyls of *Vigna angularis*. Physiol Plant **82:** 490–497

Passardi F, Penel C, Dunand C (2004) Performing the paradoxical: how plant peroxidases modify the cell wall. Trends Plant Sci **9:** 534–540

Pignocchi C, Foyer CH (2003) Apoplastic ascorbate metabolism and its role in the regulation of cell signalling. Curr Opin Plant Biol **6:** 379–389

Pitarch A, Sanchez M, Nombela C, Gil C (2002) Sequential fractionation and two-dimensional analysis unravels the complexity of the dimorphic fungi *Candida albicans* cell wall proteome. Mol Cell Proteomics **1:** 967–982

Pritchard J (1994) The control of cell expansion in roots. New Phytol **127:** 3–26

Robertson D, Mitchell GP, Gilroy JS, Gerrish C, Bolwell GP, Slabas AR (1997) Differential extraction and protein sequencing reveals major differences in patterns of primary cell wall proteins from plants. J Biol Chem **272:** 15841–15848

Rodriguez AA, Cordoba AR, Ortega L, Taleisnik E (2004) Decreased reactive oxygen species concentration in the elongation zone contributes to the reduction in maize leaf growth under salinity. J Exp Bot **55:** 1383–1390

Rodriguez AA, Grunberg KA, Taleisnik EL (2002) Reactive oxygen species in the elongation zone of maize leaves are necessary for leaf extension. Plant Physiol **129:** 1627–1632

Rodriguez AA, Lascano HR, Bustos D, Taleisnek E (2007) Salinity-induced decrease in NADPH oxidase activity in the maize leaf blade elongation zone. J Plant Physiol **164:** 223–230

Rose JKC, Braam J, Fry SC (2002) The XTH family of enzymes involved in xyloglucan endotransglucosylation and endohydrolysis: current perspectives and a new unifying nomenclature. Plant Cell Physiol **43:** 1421–1435

Saab IN, Sharp RE, Pritchard J (1992) Effect of inhibition of abscisic acid accumulation on the spatial distribution of elongation in the primary root and mesocotyl of maize at low water potentials. Plant Physiol **99:** 26–33

Saab IN, Sharp RE, Pritchard J, Voetberg GS (1990) Increased endogenous abscisic acid maintains primary root growth and inhibits shoot growth of maize seedlings at low water potentials. Plant Physiol **93:** 1329–1336

Sauter A, Dietz KJ, Hartung W (2002) A possible stress physiological role of abscisic acid conjugates in root-to-shoot signalling. Plant Cell Environ **25:** 223–228

Schroeder JI, Nambara E (2006) A quick release mechanism for abscisic acid. Cell **126:** 1023–1025

Schweikert C, Liszkay A, Schopfer P (2000) Scission of polysaccharides by peroxidase-generated hydroxyl radicals. Phytochemistry **53:** 565–570

Sharp RE (2002) Interaction with ethylene: changing views on the role of ABA in root and shoot growth responses to water stress. Plant Cell Environ **25:** 211–222

Sharp RE, Davies WJ (1979) Solute regulation and growth by roots and shoots of water-stressed maize plants. Planta **146:** 319–326

Sharp RE, Davies WJ (1989) Regulation of growth and development of plants growing with a restricted supply of water. *In* HG Jones, TL Flowers, MB Jones, eds, Plants under Stress. Cambridge University Press, Cambridge, UK, pp 72–93

Sharp RE, Hsiao TC, Silk WK (1990) Growth of the maize primary root at low water potentials. II. Role of growth and deposition of hexose and potassium in osmotic adjustment. Plant Physiol **93:** 1337–1346

Sharp RE, Poroyko V, Hejlek LG, Spollen WG, Springer GK, Bohnert HJ, Nguyen HT (2004) Root growth maintenance during water deficits: physiology to functional genomics. J Exp Bot **55:** 2343–2351

Sharp RE, Silk WK, Hsiao TC (1988) Growth of the maize primary root at low water potentials. I. Spatial distribution of expansive growth. Plant Physiol **87:** 50–57

Sharp RE, Wu Y, Voetberg GS, Saab IN, LeNoble ME (1994) Confirmation that abscisic acid accumulation is required for maize primary root elongation at low water potentials. J Exp Bot **45:** 1743–1751

Slabas AR, Ndimba B, Simon WJ, Chivasa S (2004) Proteomic analysis of the *Arabidopsis* cell wall reveals unexpected proteins with new cellular locations. Biochem Soc Trans **32:** 524–528

Spollen WG, LeNoble ME, Samuels TD, Bernstein N, Sharp RE (2000) ABA accumulation maintains primary root elongation at low water potentials by restricting ethylene production. Plant Physiol **122:** 967–976

Spollen WG, Sharp RE (1991) Spatial distribution of turgor and root growth at low water potentials. Plant Physiol **96:** 438–443

Spollen WG, Sharp RE, Saab IN, Wu Y (1993) Regulation of cell expansion in roots and shoots at low water potentials. *In* JAC Smith, H Griffiths, eds, Water Deficits: Plant Responses from Cell to Community. Bios Scientific Publishers, Oxford, pp 37–52

Sun W, Xu J, Yang J, Kieliszewski MJ, Showalter AM (2005) The lysine-rich arabinogalactan-protein subfamily in *Arabidopsis*: gene expression, glycoprotein purification and biochemical characterization. Plant Cell Physiol **46:** 975–984

Tang GQ, Luscher M, Sturm A (1999) Antisense repression of vacuolar and cell wall invertase in transgenic carrot alters early plant development and sucrose partitioning. Plant Cell **11:** 177–190

Tarpey MM, Fridovich I (2001) Methods of detection of vascular reactive species: nitric oxide, superoxide, hydrogen peroxide and peroxynitrite. Circ Res **89:** 224–236

Voigt J, Frank R (2003) 14-3-3 proteins are constituents of the insoluble glycoprotein framework of the Chlamydomonas cell wall. Plant Cell **15:** 1399–1413

Vreeburg RAM, Benschop JJ, Peeters AJM, Colmer TD, Ammerlaan AHM, Staal M, Elzenga TM, Staals RHJ, Darley CP, McQueen-Mason SJ, et al (2005) Ethylene regulates fast apoplastic acidification and expansin A transcription during submergence-induced elongation in *Rumex palustris.* Plant J **43:** 597–610

Watson BS, Lei Z, Dixon RA, Sumner LW (2004) Proteomics of *Medicago sativa* cell walls. Phytochemistry **65:** 1709–1720

Wen F, VanEtten HD, Tsaprailis G, Hawes MC (2007) Extracellular proteins in pea root tip and border cell exudates. Plant Physiol **143:** 773–783

Westgate ME, Boyer JS (1985) Osmotic adjustment and the inhibition of leaf, root, stem and silk growth at low water potentials in maize. Planta **164:** 540–549

Whetten RW, Mackay JJ, Sederoff RR (1998) Recent advances in understanding lignin biosynthesis. Annu Rev Plant Physiol Plant Mol Biol **49:** 585–609

Wu Y, Cosgrove DJ (2000) Adaptation of roots to low water potentials by changes in cell wall extensibility and cell wall proteins. J Exp Bot **51:** 1543–1553

Wu Y, Sharp RE, Durachko DM, Cosgrove DJ (1996) Growth maintenance of the maize primary root at low water potentials involves increases in cell-wall extension properties, expansin activity, and wall susceptibility to expansins. Plant Physiol **111:** 765–772

Wu Y, Spollen WG, Sharp RE, Hetherington PR, Fry SC (1994) Root growth maintenance at low water potentials: increased activity of xyloglucan endotransglycosylase and its possible regulation by abscisic acid. Plant Physiol **106:** 607–615

Wu Y, Thorne ET, Sharp RE, Cosgrove DJ (2001) Modification of expansin transcript levels in the maize primary root at low water potentials. Plant Physiol **126:** 1471–1479

Zhu J, Chen S, Alvarez S, Asirvatham VS, Schachtman DP, Wu Y, Sharp RE (2006) Cell wall proteome in the maize primary root elongation zone. I. Extraction and identification of water-soluble and lightly ionically bound proteins. Plant Physiol **140:** 311–325

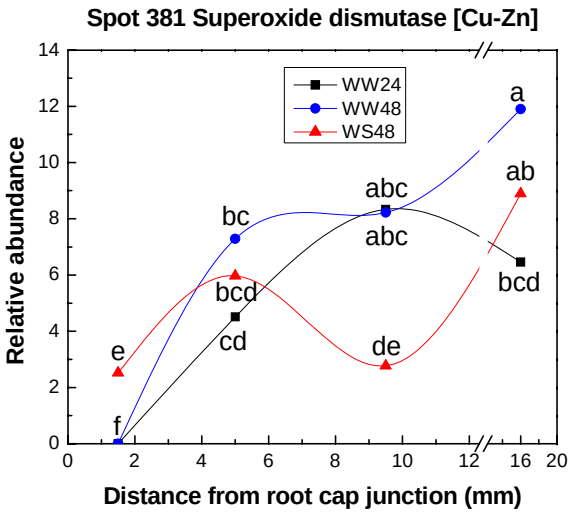

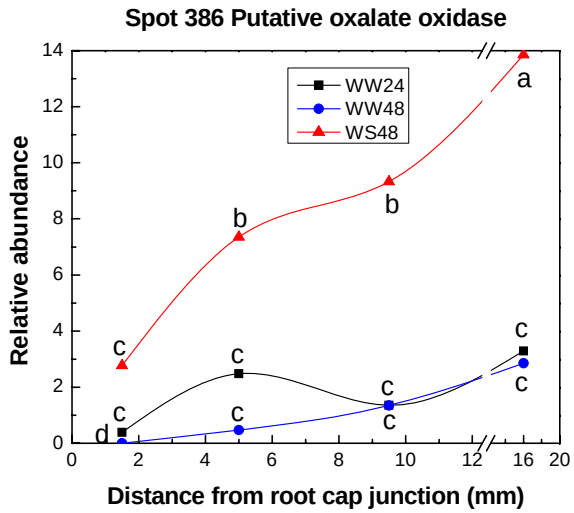

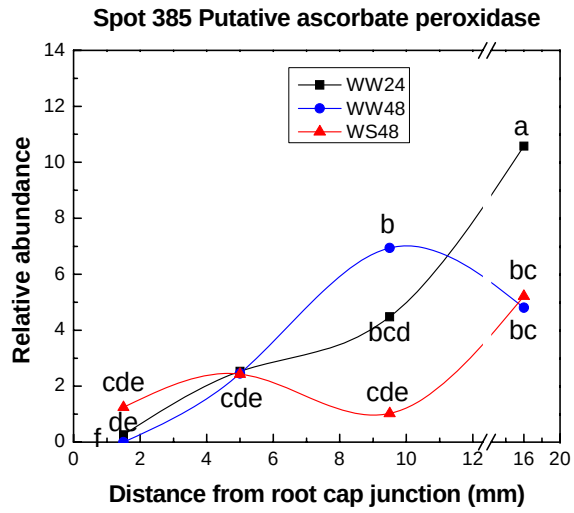

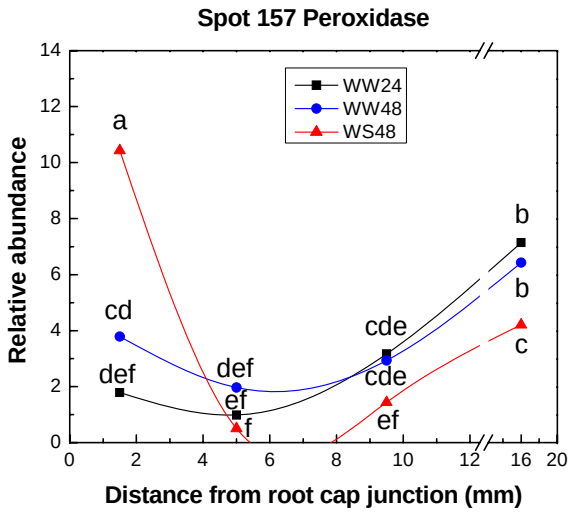

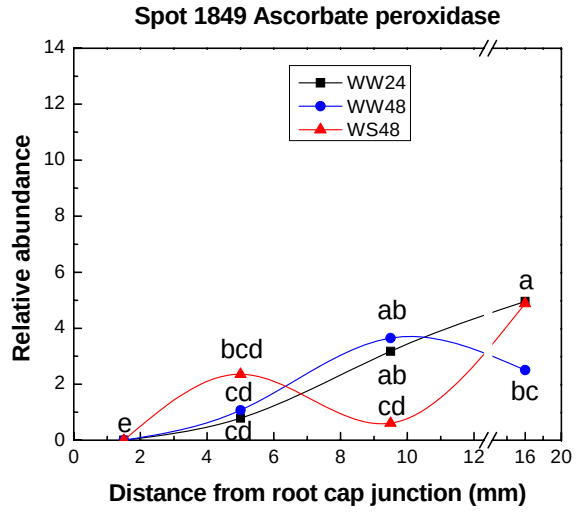

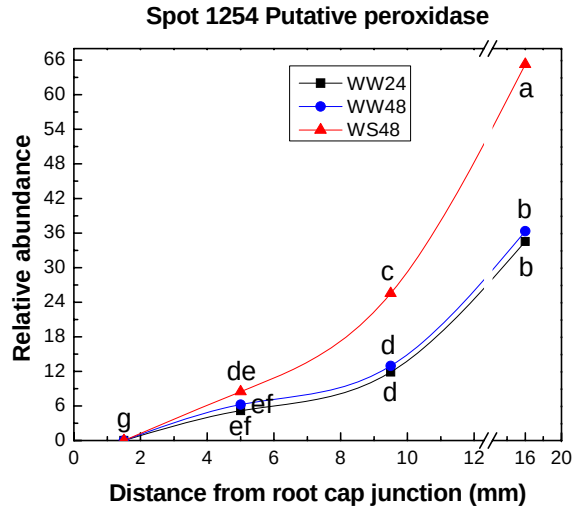

Supplemental Figure S1 (page 1 of 3)

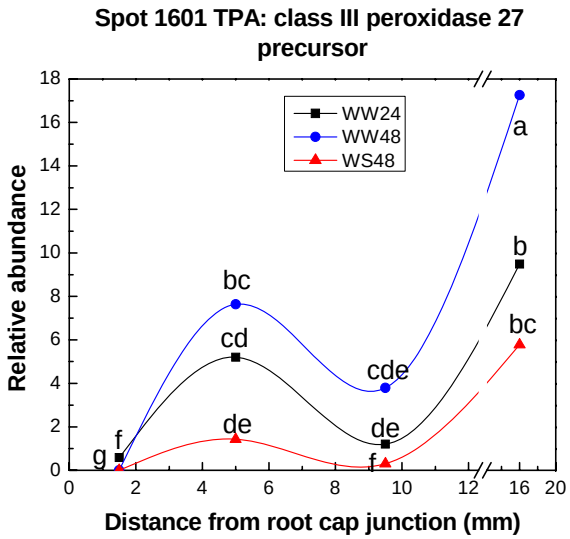
Spot 1601 TPA: class III peroxidase 27 precursor
WW24
WW48
WS48
Relative abundance
Distance from root cap junction (mm)

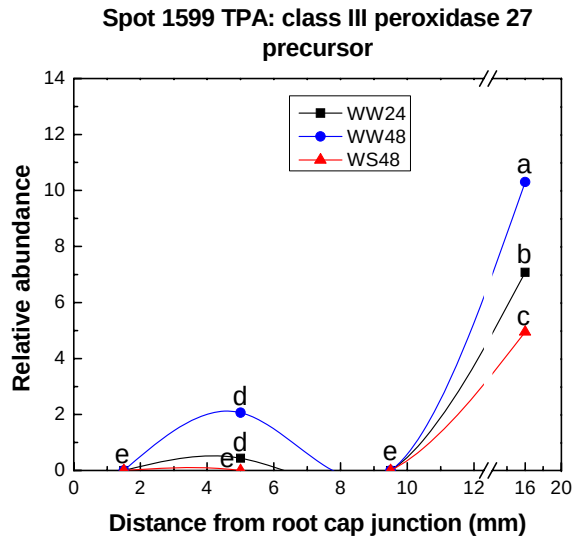
Spot 1599 TPA: class III peroxidase 27 precursor
WW24
WW48
WS48
Relative abundance
Distance from root cap junction (mm)

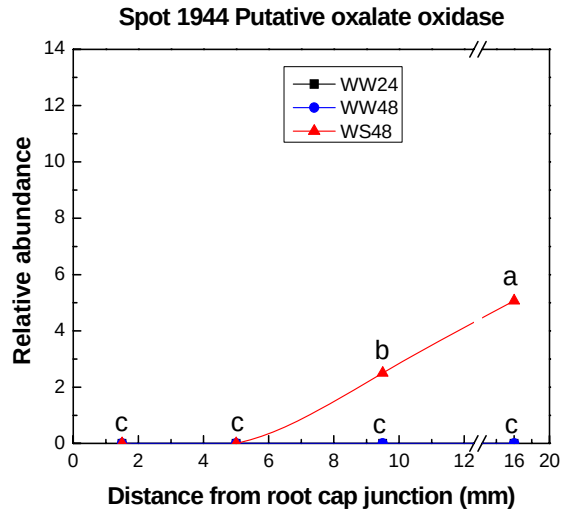
Spot 1944 Putative oxalate oxidase
WW24
WW48
WS48
Relative abundance
Distance from root cap junction (mm)

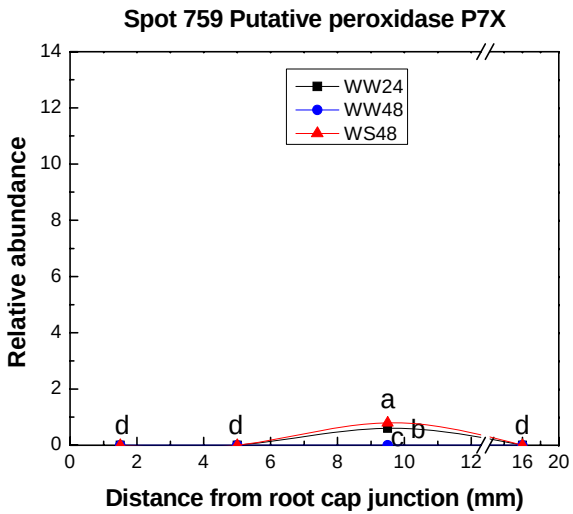
Spot 759 Putative peroxidase P7X
WW24
WW48
WS48
Relative abundance
Distance from root cap junction (mm)

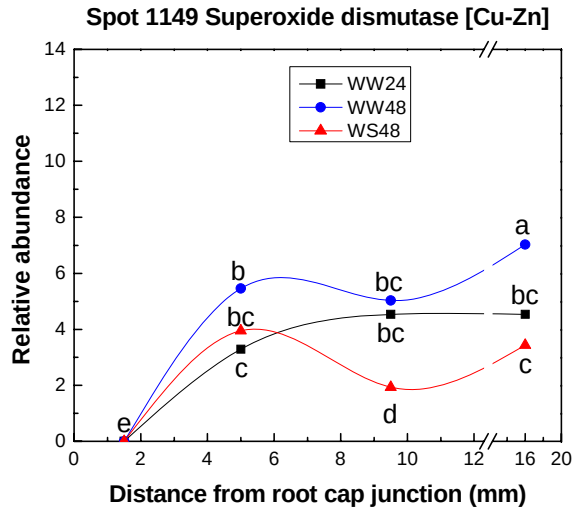
Spot 1149 Superoxide dismutase [Cu-Zn]
WW24
WW48
WS48
Relative abundance
Distance from root cap junction (mm)

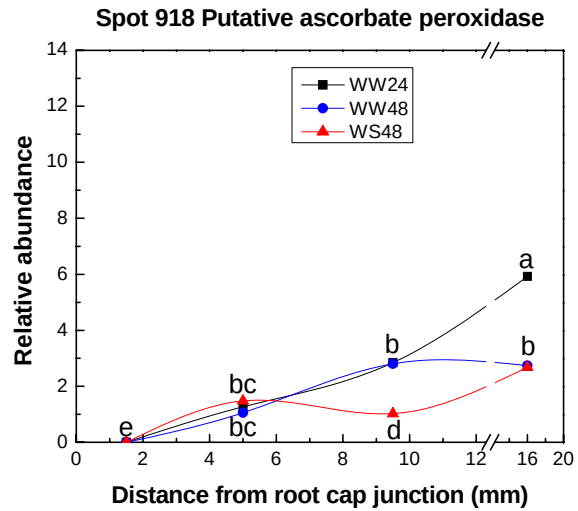
Spot 918 Putative ascorbate peroxidase
WW24
WW48
WS48
Relative abundance
Distance from root cap junction (mm)

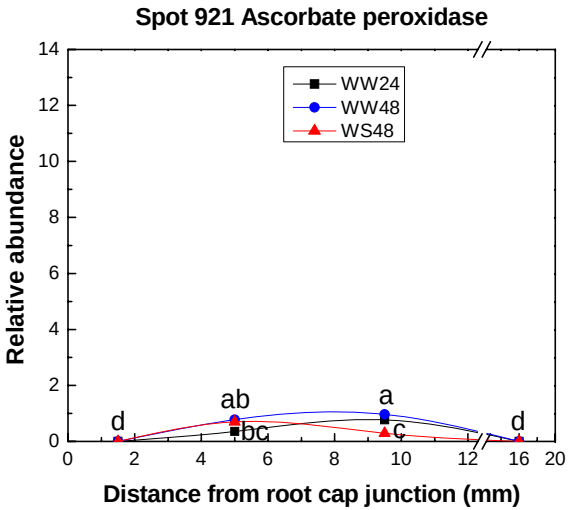
Spot 921 Ascorbate peroxidase
Relative abundance
Distance from root cap junction (mm)
WW24
WW48
WS48
d
ab
a
bc
c
d

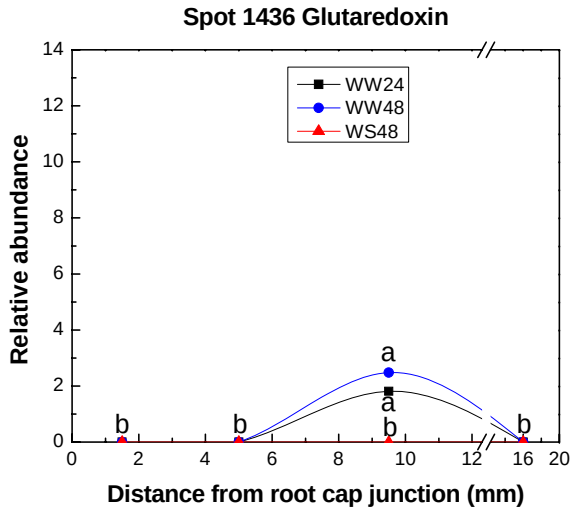
Spot 1436 Glutaredoxin
Relative abundance
Distance from root cap junction (mm)
WW24
WW48
WS48
a
b
b
a
b
b

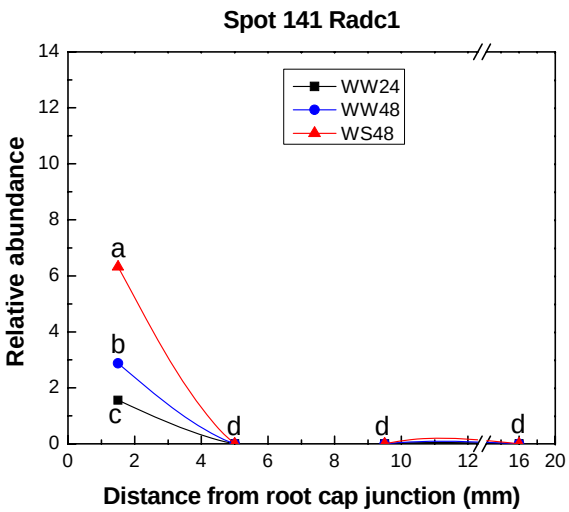

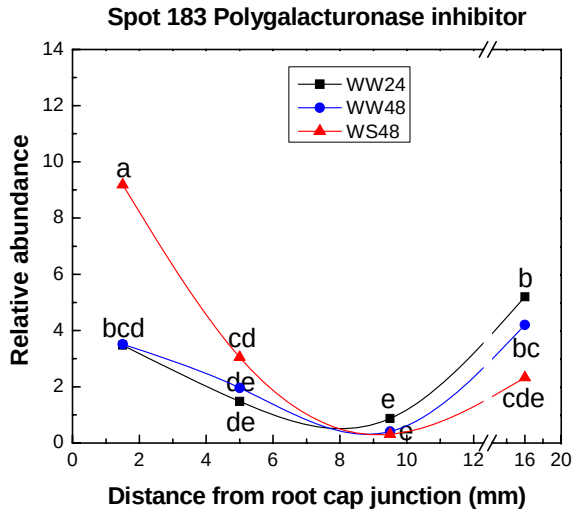

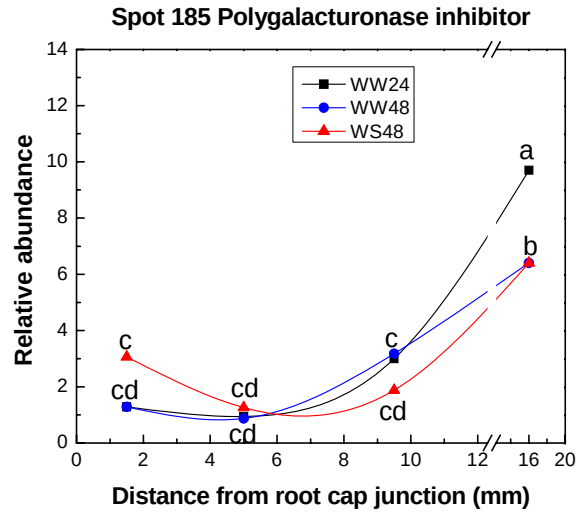

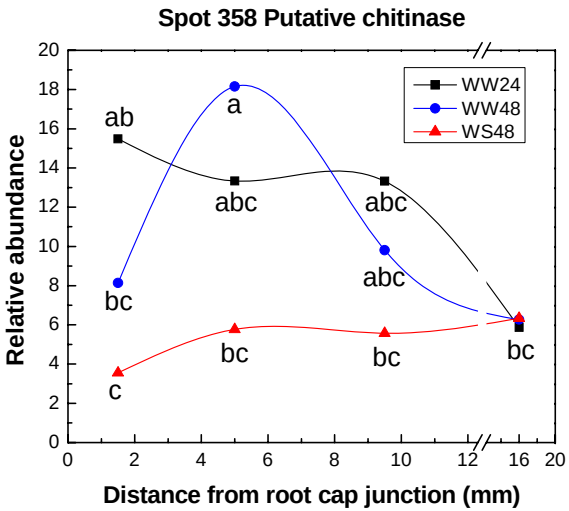

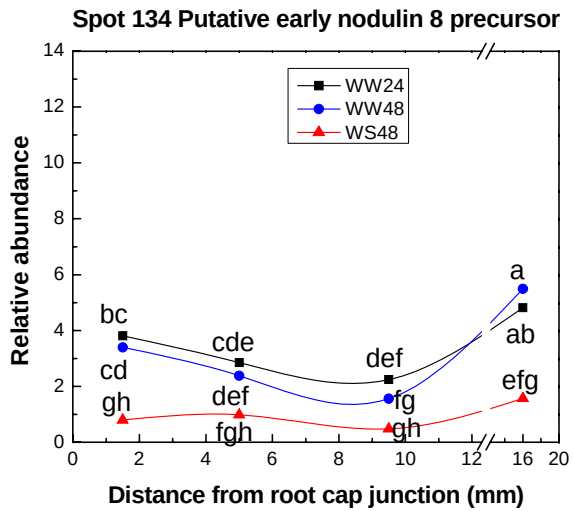

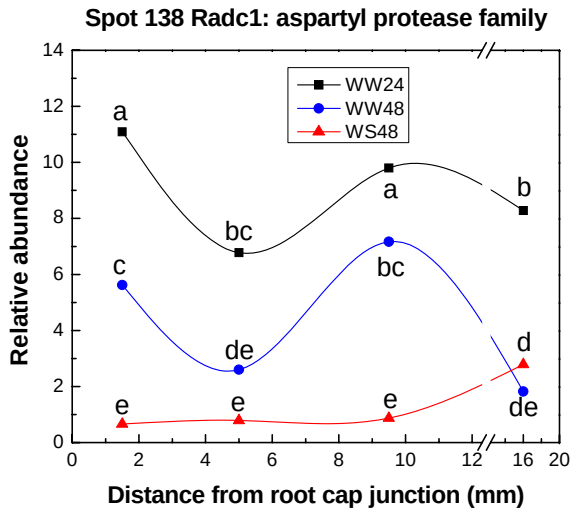

Supplemental Figure S2 (page 1 of 3)

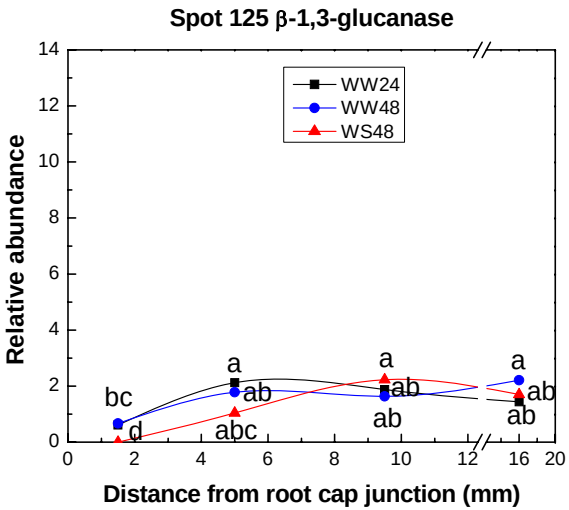

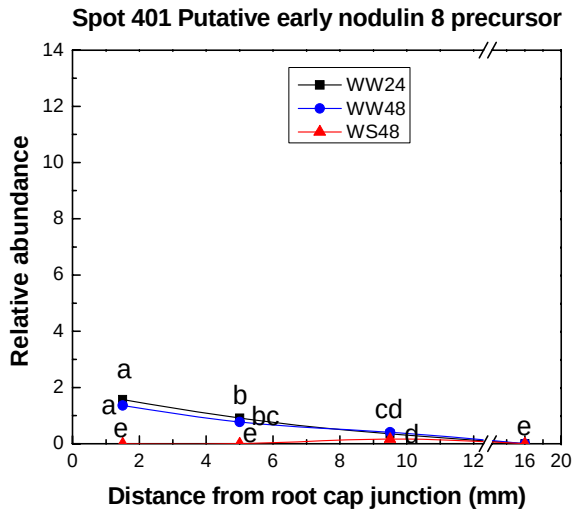

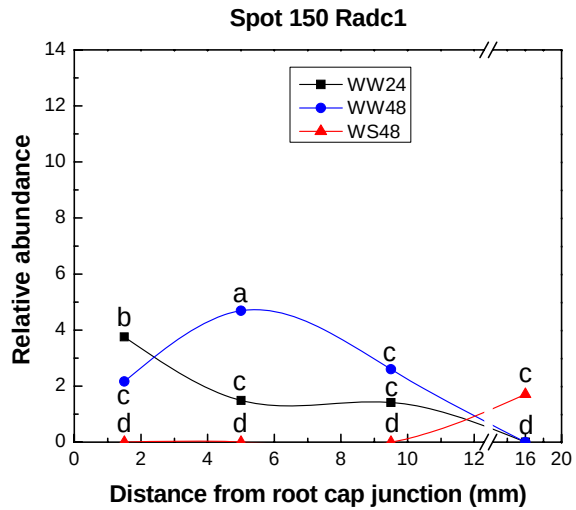

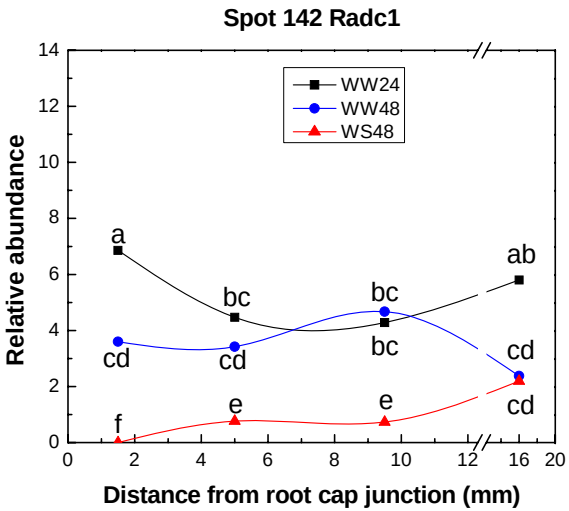

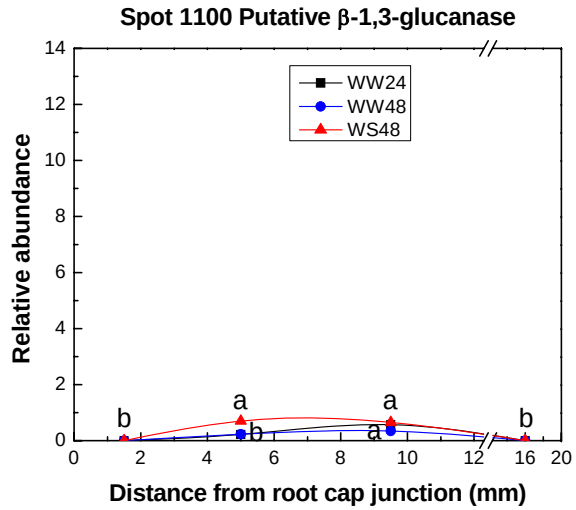

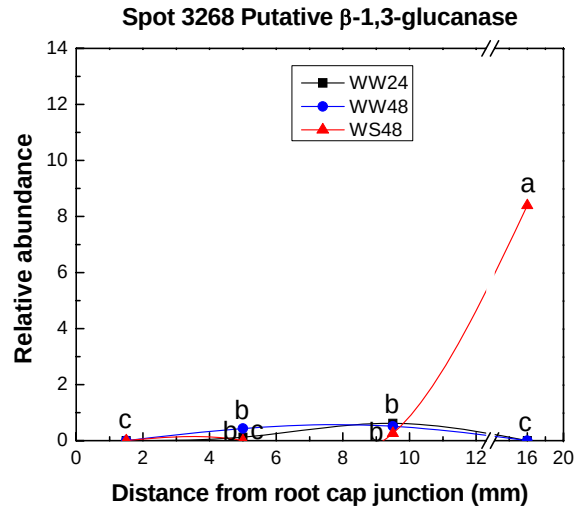

Supplemental Figure S2 (page 2 of 3)

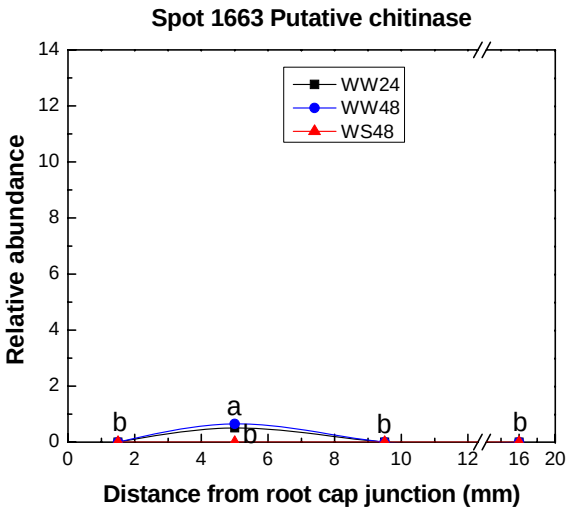

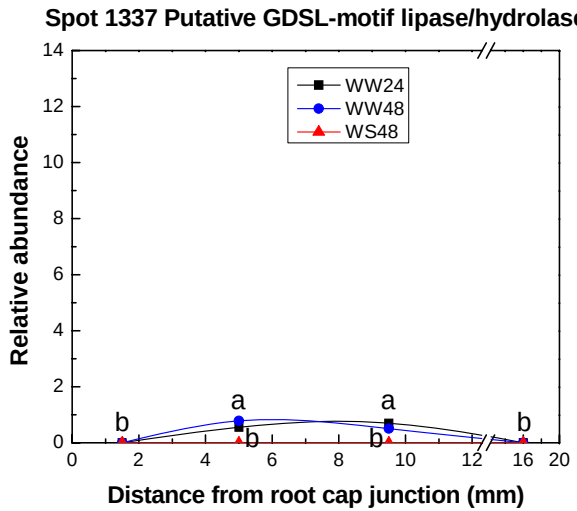

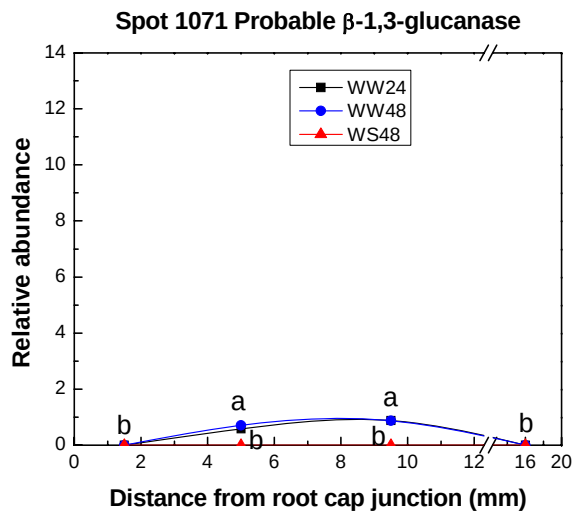

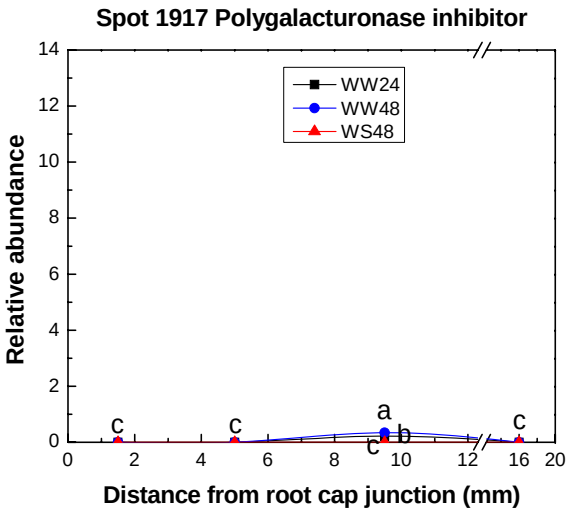

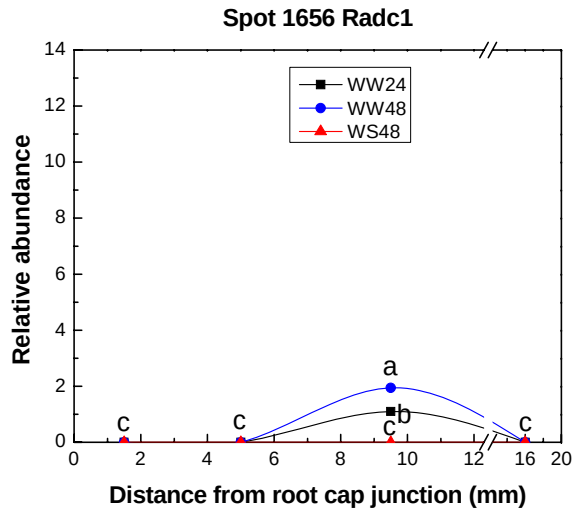

Supplemental Figure S2 (page 3 of 3)

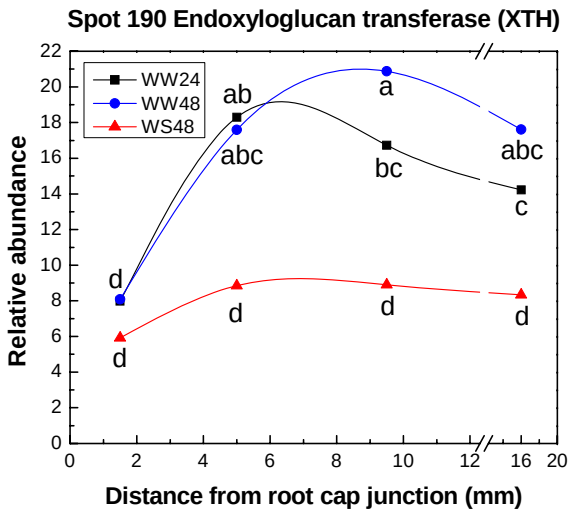

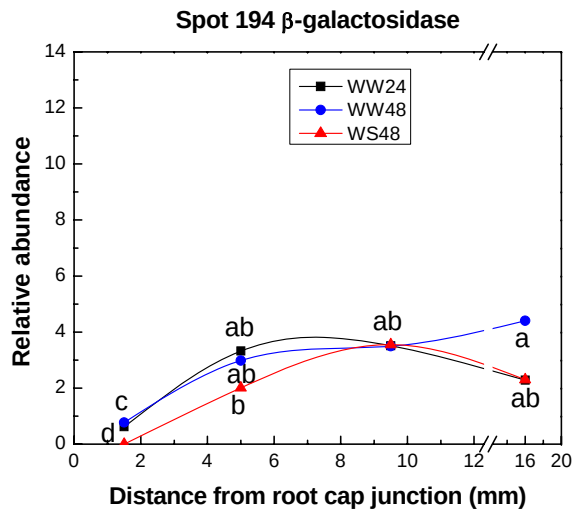

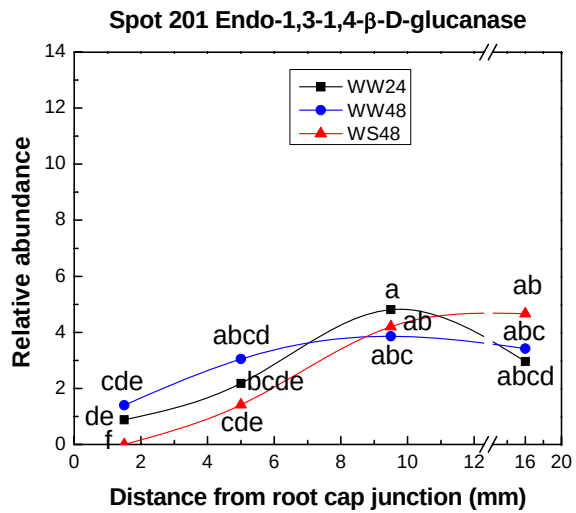

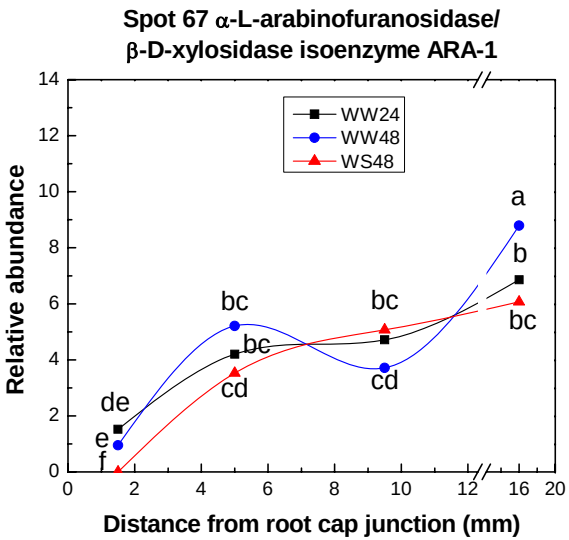

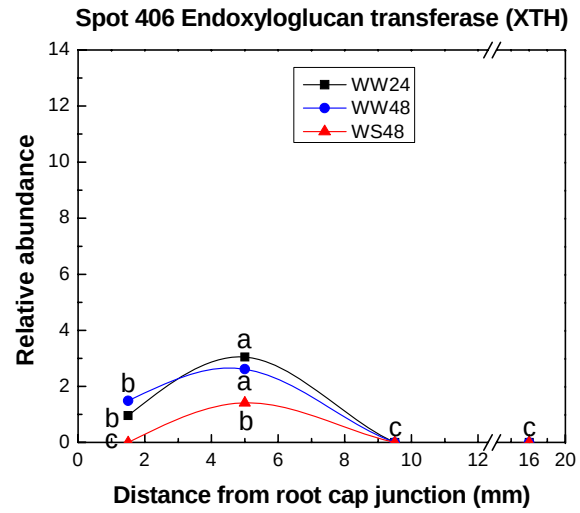

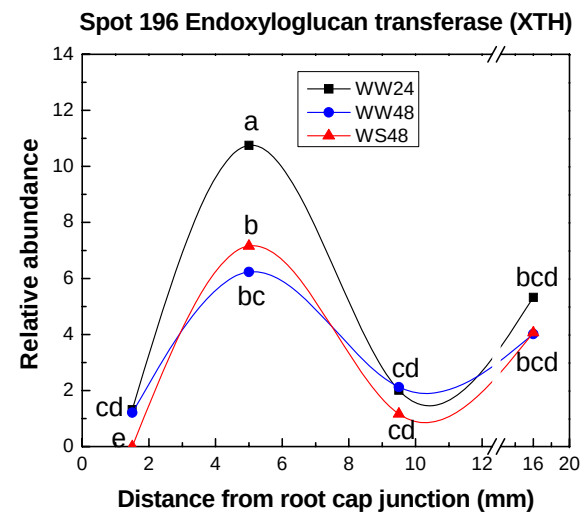

Supplemental Figure S3 (page 1 of 3)

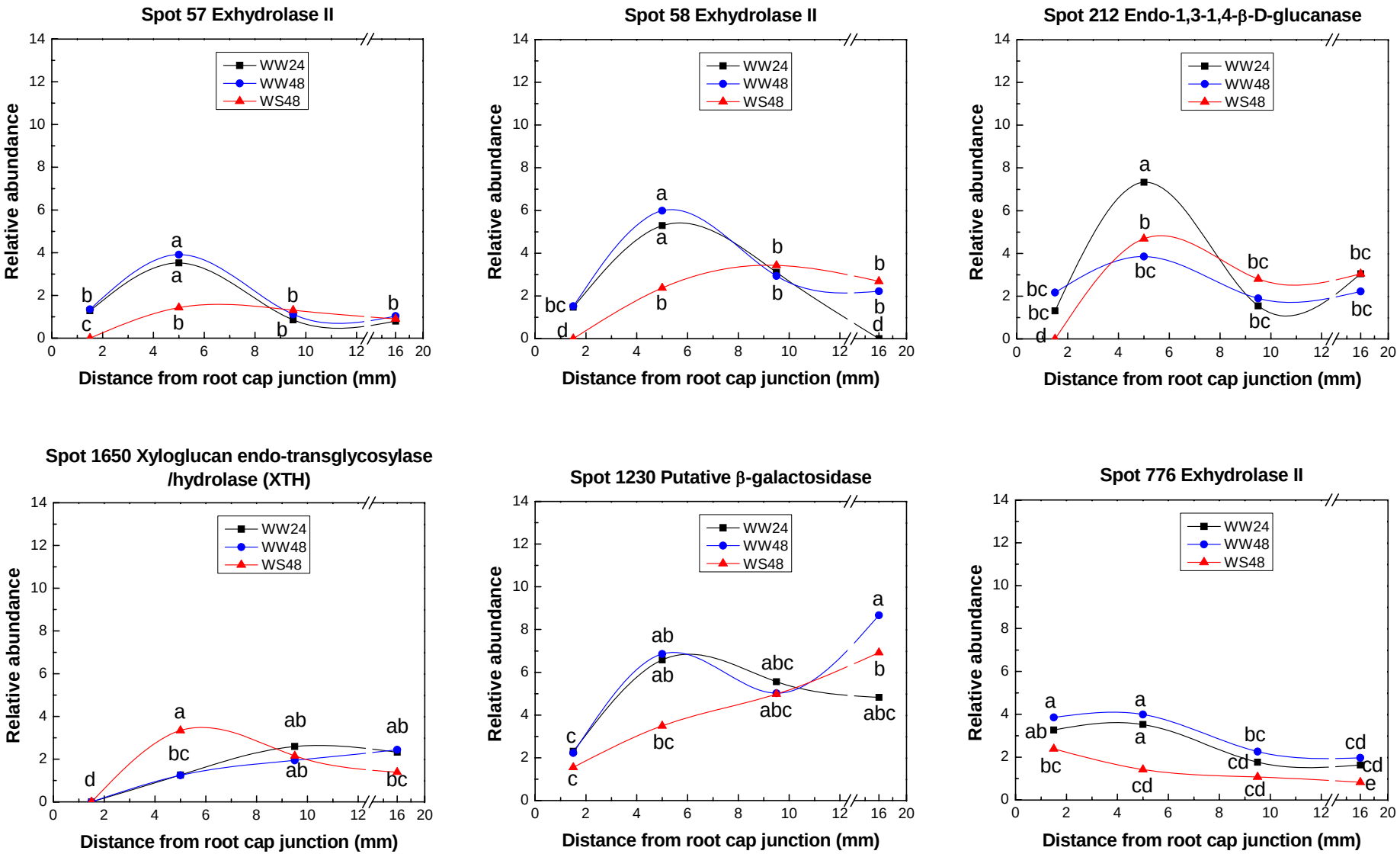

Supplemental Figure S3 (page 2 of 3)

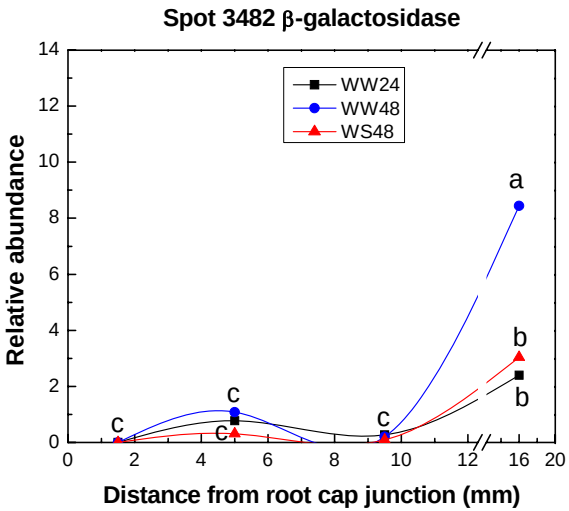

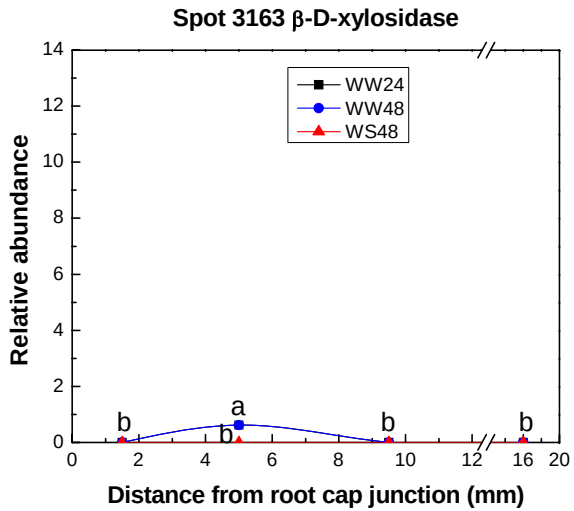

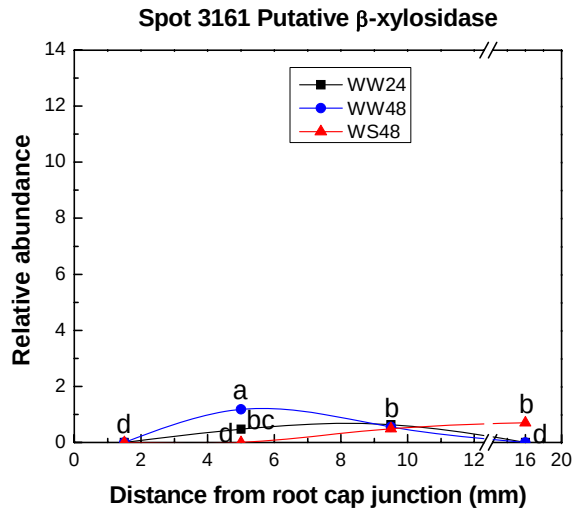

Supplemental Figure S3 (page 3 of 3)

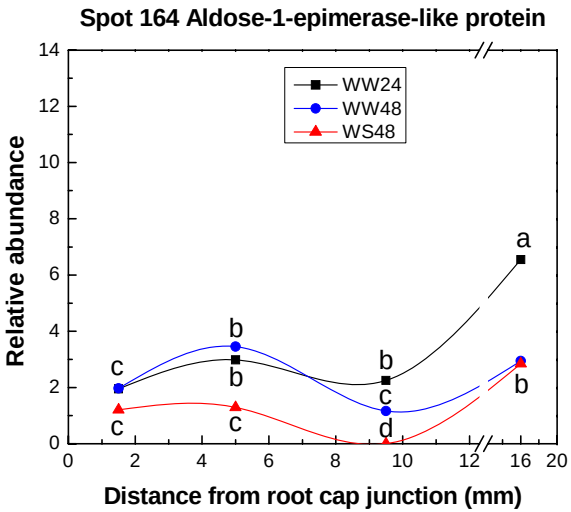

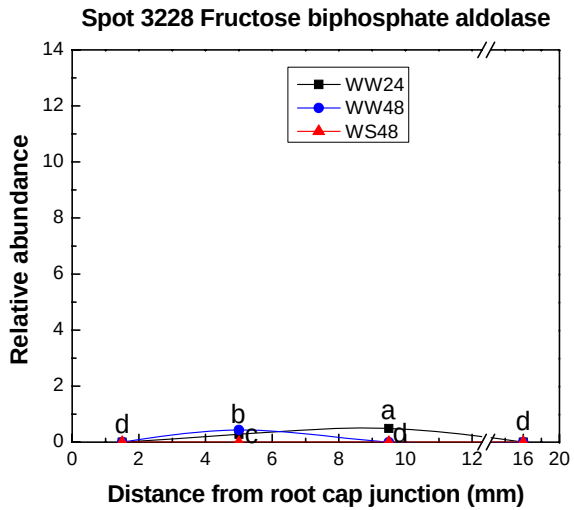

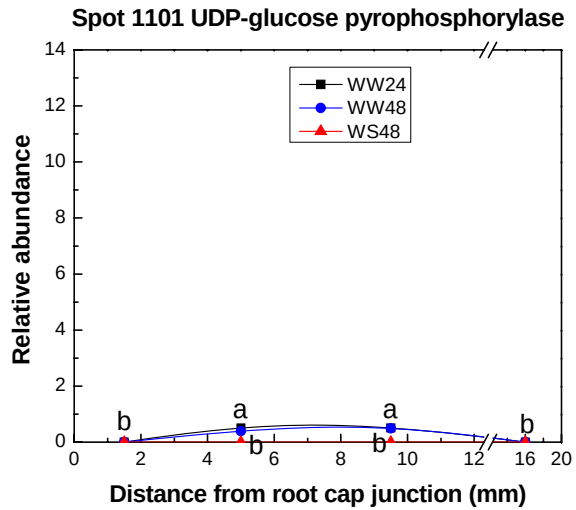

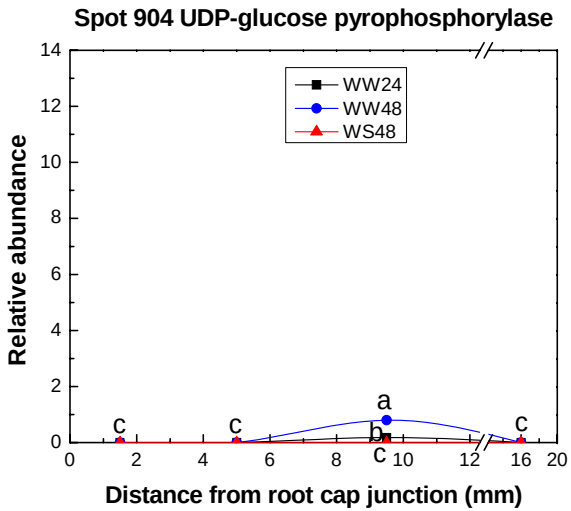

Supplemental Figure S4 (page 1 of 1)

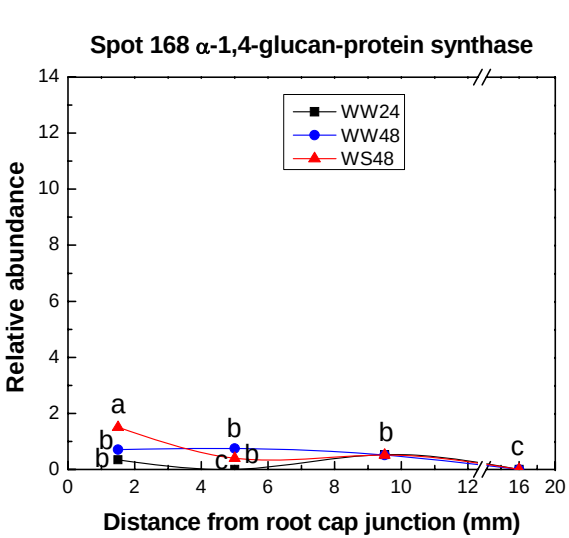

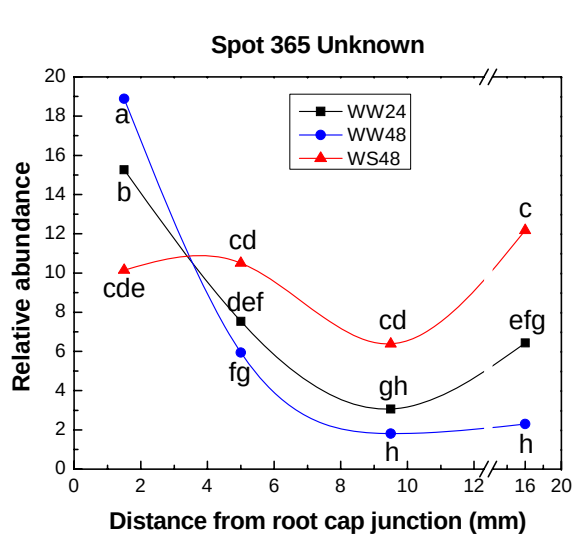

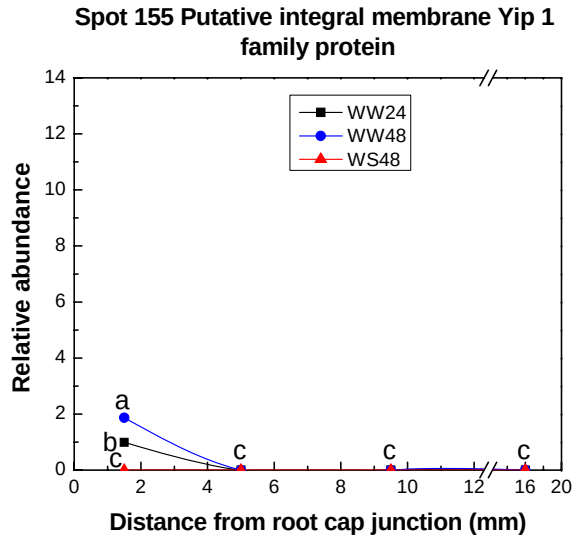

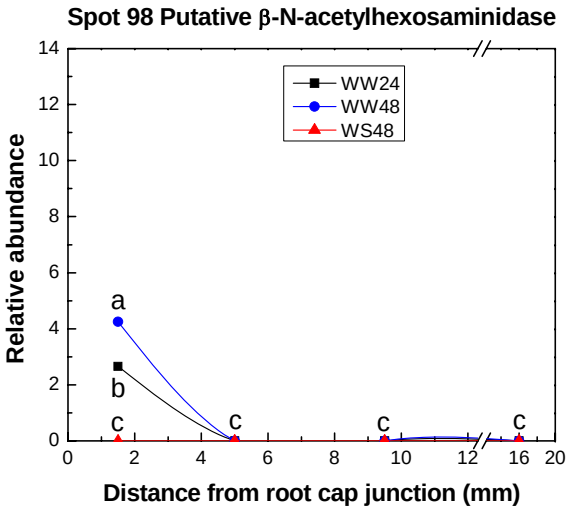

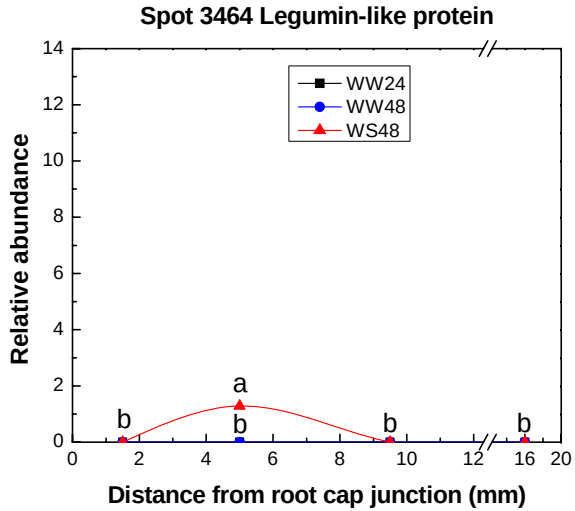

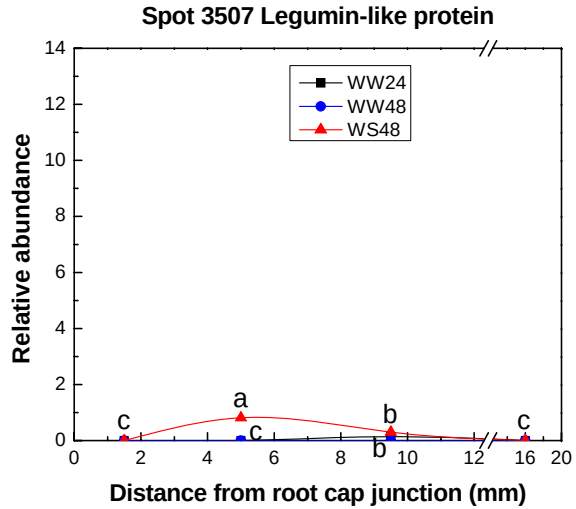

Supplemental Figure S5 (page 1 of 3)

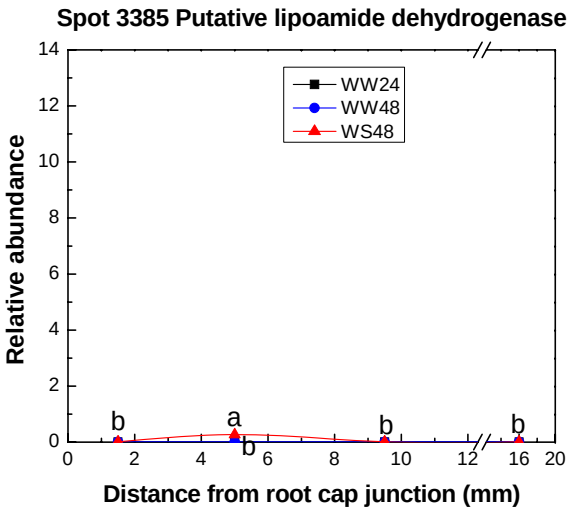

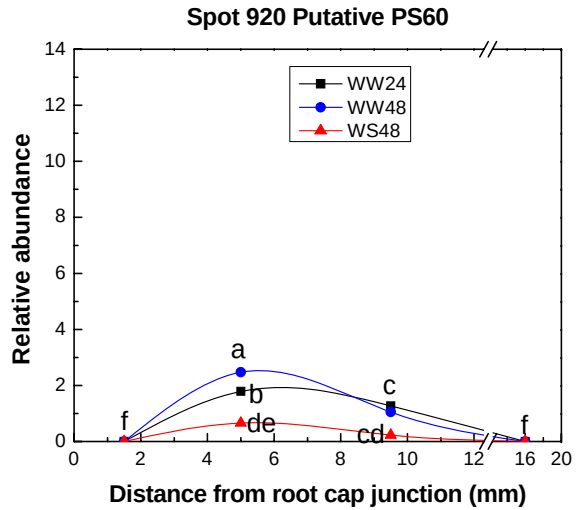

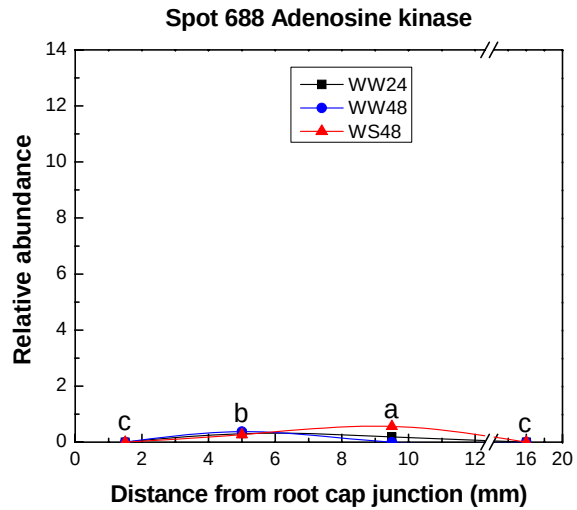

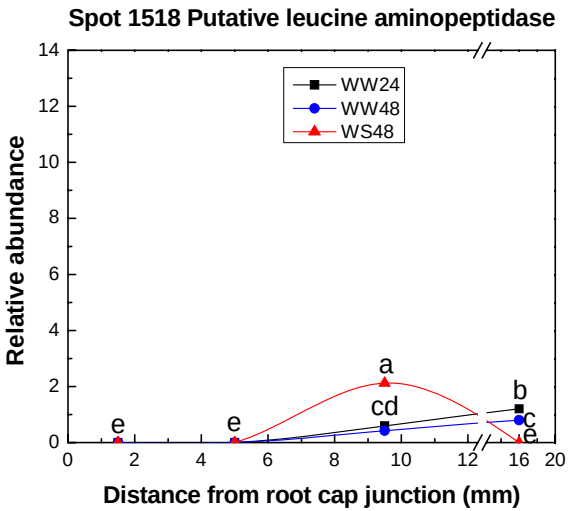

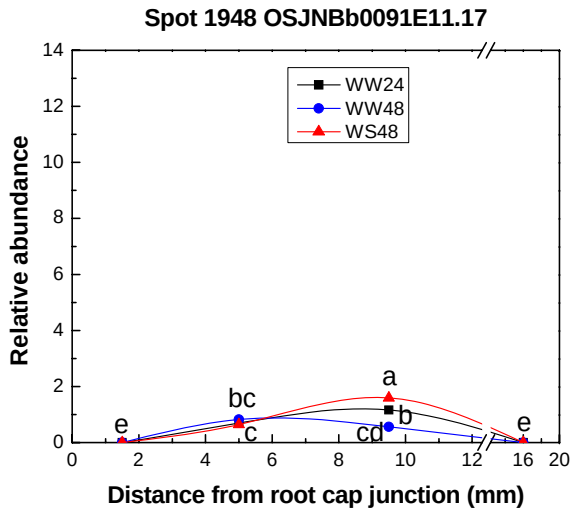

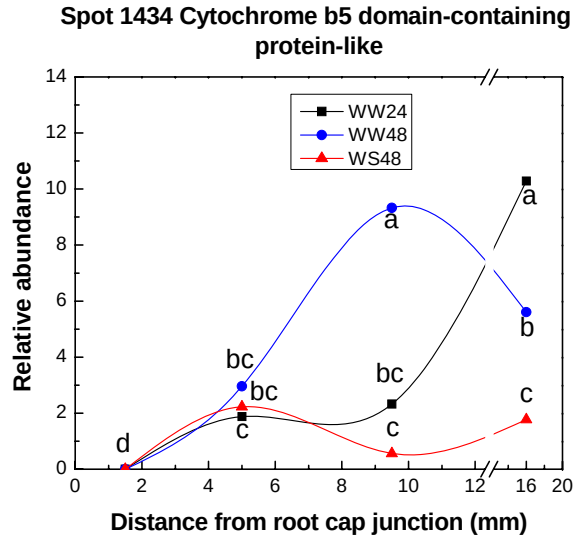

Supplemental Figure S5 (page 2 of 3)

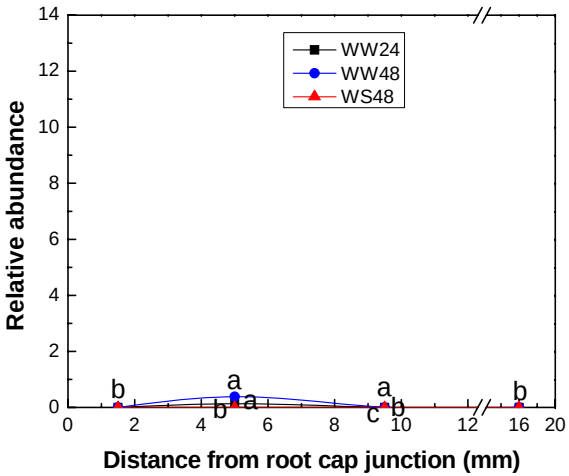
Spot 1334 Profilin 5
Relative abundance
Distance from root cap junction (mm)
WW24
WW48
WS48
0
2
4
6
8
10
12
14
16
20
b
a
b
a
c
b
a
b

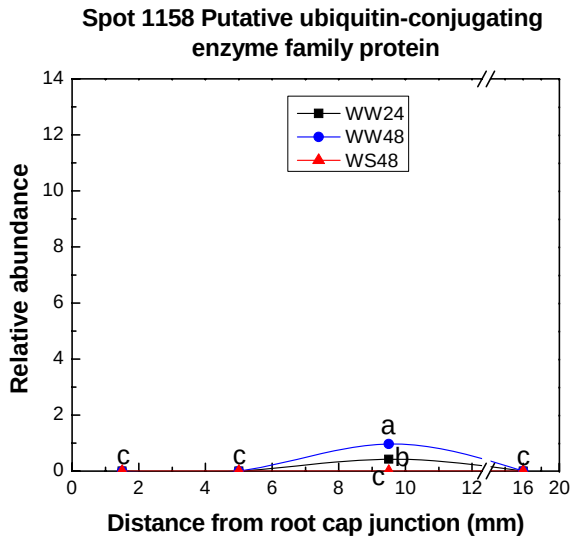
Spot 1158 Putative ubiquitin-conjugating enzyme family protein
Relative abundance
Distance from root cap junction (mm)
WW24
WW48
WS48
0
2
4
6
8
10
12
14
16
20
c
c
a
b
c
c

Supplemental Figure S1. Spatial distribution of protein abundance for 14 fraction 1 CWPs in the category of ROS metabolism in the apical 20 mm of primary roots grown under well-watered (water potential of -0.03 MPa) or water-stressed (water potential of -1.6 MPa) conditions. Well-watered roots were harvested at 24 h (WW24; developmental control, roots of the same length as water-stressed roots) and 48 h (WW48; temporal control, roots of the same age as water-stressed roots) after transplanting. Water-stressed roots were harvested at 48 h after transplanting (WS48). Three replicates were analyzed for each treatment. The fitted lines were smoothed using the SPLINE method. Different letters indicate significant differences at the $P<0.05$ level. The panels are presented from left to right in the same order as the listing of proteins in Figure 5 of the main body of the paper.

Supplemental Figure S2. Spatial distribution of protein abundance for 17 fraction 1 CWPs in the category of defense and detoxification in the apical 20 mm of primary roots grown under well-watered or water-stressed conditions. See the legend for Supplemental Figure S1 for full description. The panels are presented from left to right in the same order as the listing of proteins in Figure 6 of the main body of the paper.

Supplemental Figure S3. Spatial distribution of protein abundance for 15 fraction 1 CWPs in the category of hydrolases in the apical 20 mm of primary roots grown under well-watered or water-stressed conditions. See the legend for Supplemental Figure S1 for full description. The panels are presented from left to right in the same order as the listing of proteins in Figure 7 of the main body of the paper.

Supplemental Figure S4. Spatial distribution of protein abundance for four fraction 1 CWPs in the category of carbohydrate metabolism in the apical 20 mm of primary roots grown under well-watered or water-stressed conditions. See the legend for Supplemental Figure S1 for full description. The panels are presented from left to right in the same order as the listing of proteins in Figure 8 of the main body of the paper.

Supplemental Figure S5. Spatial distribution of protein abundance for 14 fraction 1 CWPs in the category of other/unknown in the apical 20 mm of primary roots grown under well-watered or water-stressed conditions. See the legend for Supplemental Figure S1 for full description. The panels are presented from left to right in the same order as the listing of proteins in Figure 9 of the main body of the paper.

Supplemental Video S1. Consecutive focal planes (each 3 μm in thickness) of the merged confocal image from R1 (approximately 1.5 mm from the apex) of a water-stressed root presented in Figure 12 of the main body of the paper. The root was stained for apoplastic ROS using H_2DCF (green fluorescence) and with the membrane probe FM 1-43 (red fluorescence) to visualize the cellular structure. In contrast to the apoplastic localization of ROS staining with H_2DCF in the root epidermis, several detached and mature root cap cells showed cytoplasmic and nuclear staining with H_2DCF.

Supplemental Table S1. *Identities of water deficit-responsive protein spots from the 2-DE gels of water soluble and lightly ionically-bound (fraction 1) CWPs*

Spots were identified by HPLC-electrospray quadrupole time-of-flight mass spectrometry, and proteins were classified in five functional categories. SP refers to the presence of a signal peptide sequence predicted by SignalP (v3) with a P value threshold greater than 0.900. NSP indicates non-classical secretory proteins predicted by SecretomeP 1.0b (http://www.cbs.dtu.dk/services/SecretomeP-1.0) with an NN score greater than 0.600. Identifications and accession numbers (protein GI number) are from the National Center for Biotechnology Information (NCBI) database. The score, number of matched peptides and percent coverage are taken directly from the Mascot Daemon report. Theoretical molecular mass (in kD) and pI were estimated based on the top protein sequence obtained by BLASTX. Proteins were identified from R1 to R3 in the present study or by image cross comparison with the master gels (MG) in Zhu et al. (2006). Protein spots from R4 were not used for identifications. Protein identifications marked with an asterisk are one of the multiple protein identifications obtained for that spot number.

Spot No.	Identification	Experimental Mass	Experimental pI	Theoretical Mass	Theoretical pI	Accession No.	Mascot Score	No. of Peptides	Coverage %	SP	NSP	Identified from Region(s)	Organism Matched
	ROS metabolism												
157	Peroxidase	39	8.2	36	8.0	25044849	151	3	10	x		R3	*Ananas comosus*
176	Malate dehydrogenase*	37	6.3	35	8.7	19880701	147	3	12			R1	*Oryza sativa*
176	Putative peroxidase 1 precursor*	37	6.3	35	7.3	52076453	168	3	13	x		R1	*Oryza sativa*
177	Class III peroxidase 80 precursor	37	6.6	34	6.9	55701027	177	3	26	x		R1	*Oryza sativa*
218	Cationic peroxidase isozyme 40K precursor	24	6.7	36	8.7	575605	60	3	12	x		R1	*Nicotiana tabacum*
354	Cationic peroxidase isozyme 40K precursor	36	9.2	36	8.7	575605	431	8	36	x		R1	*Nicotiana tabacum*
381	Superoxide dismutase [Cu-Zn]	17	5.9	15	5.6	134598	89	4	23	x		MG spot 45	*Zea mays*
385	Putative ascorbate peroxidase	25	5.5	27	5.4	50920595	274	6	20	x		R1	*Oryza sativa*
386	Putative oxalate oxidase	23	5.6	24	9.0	50917909	135	2	8	x		R1 R2	*Oryza sativa*
395	Probable germin protein 4	23	6.8	22	7.8	34902528	128	2	11	x		R1	*Oryza sativa*
547	Putative peroxidase	47	7.3	40	7.2	50939495	173	3	20	x		R3	*Oryza sativa*
735	Putative peroxidase P7X*	36	5.1	34	6.9	15011986	116	2	7	x		R3	*Oryza sativa*
759	Putative peroxidase P7X	34	7.5	34	6.9	15011986	58	2	8	x		R3	*Zea mays*
918	Putative ascorbate peroxidase*	26	5.2	27	5.4	50920595	170	4	12	x		R3	*Oryza sativa*
921	Ascorbate peroxidase*	26	5.1	27	5.5	2997688	79	3	15	x		R3	*Zantedeschia aethiopica*
1149	Superoxide dismutase [Cu-Zn]	17	5.6	15	5.6	4753356	83	4	18		x	MG spot 48	*Zea mays*
1254	Putative peroxidase	40	3.9	36	4.7	31429827	224	4	11	x		R2	*Oryza sativa*
1436	Glutaredoxin	11	8.3	12	7.1	485953	348	4	44			R3	*Oryza sativa*
1599	TPA: class III peroxidase 27 precursor	31	7.0	33	8.4	55700921	149	4	18	x		R2	*Oryza sativa*
1601	TPA: class III peroxidase 27 precursor	31	8.2	33	8.4	55700921	465	9	43	x		R2	*Oryza sativa*
1663	Putative germin-like protein*	28	8.0	24	8.5	50251393	132	2	24	x		R2	*Oryza sativa*
1849	Ascorbate peroxidase	25	5.4	20	7.5	56412205	66	3	14	x		R3	*Pennisetum glaucum*
1902	TPA: class III peroxidase 27 precursor *	34	8.1	33	8.1	55700921	150	3	9	x		R3	*Oryza sativa*
1944	Putative oxalate oxidase	22	5.6	24	9.0	50917909	121	2	11	x		R3	*Oryza sativa*
3185	Thioredoxin h *	11	4.1	13	4.9	12082335	63	2	15		x	R2	*Oryza sativa*
3336	TPA: class III peroxidase 27 precursor	15	4.6	33	8.4	55700921	68	2	5	x		R2	*Oryza sativa*

3464	Malate dehydrogenase*	35	5.9	35	8.7	19880701	112	2	6			R2	*Oryza sativa*
3465	Putative purple acid phosphatase*	34	6.0	37	5.3	31429892	143	3	10	x		R2	*Oryza sativa*
3505	Probable germin protein 4*	23	6.5	22	7.8	34902528	203	3	18	x		R2	*Oryza sativa*
3505	Putative ascorbate peroxidase*	23	6.5	27	5.4	50920595	137	3	12		x	R2	*Oryza sativa*
	Defense and detoxification												
50	Putative Bplo*	79	6.1	65	6.1	34897712	52	2	4	x		R1	*Oryza sativa*
74	Putative syringolide-induced protein B13-1-1*	72	7.7	63	7.7	50899710	183	5	10	x		R1	*Oryza sativa*
125	β-1,3-glucanase	51	5.8	49	6.3	924953	197	4	10	x		R1	*Triticum aestivum*
134	Putative early nodulin 8 precursor	45	7.5	42	7.3	50938787	471	10	29	x		R1 R2 R3	*Oryza sativa*
138	Radc1:aspartyl protease family	44	7.9	45	6.9	32972250	109	4	4	x		MG spot 19	*Oryza sativa*
141	Radc1	45	8.6	45	7.1	49532749	118	3	9	x		R1	*Oryza sativa*
142	Radc1	44	7.3	45	7.1	49532749	409	8	20	x		R1 R3	*Oryza sativa*
150	Radc1	44	7.7	45	7.1	49532749	261	5	14	x		R1 R3	*Oryza sativa*
183	Polygalacturonase inhibitor protein	36	7.8	36	7.5	18148925	486	8	25	x		R1	*Citrus sp. cv. Sainum*
185	Polygalacturonase inhibitor protein	36	7.3	36	7.5	18148925	575	10	45	x		R1	*Citrus sp. cv. Sainum*
190	Polygalacturonase inhibitor protein*	34	6.8	36	7.5	18148925	133	3	9	x		R1	*Citrus sp. cv. Sainum*
216	γ-glutamyl transpeptidase	25	6.8	61	9.5	928934	97	3	14	x		R1	*Arabidopsis thaliana*
244	Putative dirigent protein*	12	4.5	20	8.7	42454402	93	2	22	x		R1	*Saccharum officinarum*
358	Putative chitinase	28	8.6	32	6.5	55168113	380	7	24	x		R1	*Oryza sativa*
401	Putative early nodulin 8 precursor	45	6.9	42	7.3	50938787	242	4	24	x		R1	*Oryza sativa*
402	Putative early nodulin 8 precursor*	43	6.9	42	7.3	50938787	273	6	18	x		R1	*Oryza sativa*
402	Radc1*	43	6.9	45	7.1	49532749	244	5	14	x		R1 R3	*Oryza sativa*
407	Polygalacturonase inhibitor protein	34	7.1	36	7.5	18148925	183	4	16	x		R1	*Citrus sp. cv. Sainum*
735	Putative phytocyanin protein, PUP2*	36	5.1	27	5.2	52076874	102	2	7	x		R3	*Oryza sativa*

820	Glyoxalase I	32	5.7	32	5.6	37932483	138	3	9			R3	*Zea mays*
840	Putative class III chitinase RCB4	31	4.6	34	5.2	31432078	44	2	5	x		R3	*Oryza sativa*
1071	Probable β-1,3-glucanase	50	5.6	49	6.3	7489680	147	3	6	x		R3	*Triticum aestivum*
1100	Putative β-1,3-glucanase	51	5.1	53	5.2	50905193	157	2	6	x		R2	*Oryza sativa*
1257	Osmotin	15	8.7	18	7.9	21207583	171	8	29	x		MG spot 46	*Pennisetum ciliare*
1334	Putative disease resistance response protein-related*	14	4.4	24	8.5	34899372	125	2	22	x		R3	*Oryza sativa*
1337	Putative GDSL-motif lipase/hydrolase	39	7.8	39	8.5	34907922	86	3	8	x		R3	*Oryza sativa*
1656	Radc1	46	8.0	45	7.1	49532749	377	7	19	x		R3	*Oryza sativa*
1663	Putative chitinase*	28	8.0	24	6.5	55168113	132	2	17	x		R2	*Oryza sativa*
1739	Lactoylglutathione lyase	14	5.6	15	6.5	40336524	141	7	32		x	MG spot 50	*Arabidopsis thaliana*
1917	Polygalacturonase inhibitor protein	23	6.4	36	8.4	1143381	103	2	9	x		R3	*Actinidia deliciosa*
2669	Cysteine proteinase inhibitor	11	5.1	15	5.9	809608	81	2	29	x		R2	*Zea mays*
3185	P0463A02.21*	11	4.1	17	5.3	34895198	61	2	22		x	R2	*Oryza sativa*
3214	Glyoxalase I*	32	5.2	32	5.6	37932483	96	2	20			R2	*Zea mays*
3268	Putative β-1,3-glucanase	34	4.3	48	4.9	31126737	118	2	8	x		R2	*Oryza sativa*
3420	Putative Bplo*	76	5.8	66	6.1	34897712	189	3	7	x		R2	*Oryza sativa*
	Hydrolases												
53	Exhydrolase II*	78	6.9	68	6.6	4731111	201	4	8	x		R1	*Zea mays*
57	Exhydrolase II	77	6.5	68	6.6	4731111	140	3	8	x		R1	*Zea mays*
58	Exhydrolase II*	78	6.8	68	6.6	4731111	192	5	11	x		R1	*Zea mays*
62	Exhydrolase II*	76	7.4	68	6.6	4731111	167	3	6	x		R1	*Zea mays*
64	Exhydrolase II	76	6.3	68	6.6	4731111	100	2	5	x		R1	*Zea mays*
67	α-L-arabinofuranosidase/β-D-xylosidase isoenzyme ARA-1	71	5.2	82	5.9	18025340	70	2	6	x		R1	*Hordeum vulgare*
97	β-D-glucosidase	59	5.6	64	6.2	4096602	362	7	15			R1	*Zea mays*
98	β-D-glucosidase*	60	6.2	64	6.2	4096602	56	2	5			R1	*Zea mays*
99	β-D-glucosidase	61	5.7	64	6.2	4096602	661	13	28			R1 R2	*Zea mays*
170	Putative α-galactosidase preproprotein	39	6.1	46	8.1	31432825	264	5	14	x		R1	*Oryza sativa*
171	Putative α-galactosidase preproprotein	38	5.8	46	8.1	31432825	158	5	14	x		R1	*Oryza sativa*

190	Endoxyloglucan transferase (XTH)*	34	6.0	34	6.4	1885310	422	10	27	x		R1	*Hordeum vulgare*
194	β-galactosidase	32	5.4	89	6.6	33521218	47	2	9	x		R1	*Sandersonia aurantia*
196	Endoxyloglucan transferase (XTH)	32	6.8	34	6.4	1885310	407	9	33	x		R1	*Hordeum vulgare*
201	Endo-1,3-1,4-β-D-glucanase	29	7.0	33	7.2	3822036	189	4	17	x		R1	*Zea mays*
212	Endo-1,3-1,4-β-D-glucanase	28	6.7	33	7.2	3822036	243	3	27	x		R1	*Zea mays*
301	β-D-glucosidase	58	5.5	64	6.2	4096602	122	4	7			R1	*Zea mays*
302	Exhydrolase II	77	6.7	68	6.6	4731111	178	3	5	x		R3	*Zea mays*
335	β-glucosidase	56	9.0	57	9.0	50918079	224	5	10	x		R1	*Oryza sativa*
343	β-xylosidase-like protein	71	5.7	87	6.4	7671447	100	2	2	x		R3	*Arabidopsis thaliana*
400	β-D-glucosidase	58	5.3	64	6.2	4096602	208	6	12			R1	*Zea mays*
406	Endoxyloglucan transferase (XTH)	35	7.1	34	6.4	1885310	186	5	18	x		R1	*Hordeum vulgare*
409	β-D-glucosidase*	58	5.2	64	6.2	4096602	228	6	4			R1 R2 R3	*Zea mays*
422	β-glucosidase	59	5.4	65	6.2	435313	42	5	8			MG spot 57	*Zea mays*
776	Exhydrolase II	72	6.9	68	6.6	4731111	330	5	11	x		R2	*Zea mays*
920	Endoxyloglucan transferase (XTH)*	60	6.8	34	6.4	1885310	155	4	13	x		R2	*Hordeum vulgare*
1041	β-D-glucosidase	53	5.6	64	6.2	4096602	135	4	7			R2	*Zea mays*
1230	Putative β-galactosidase	43	6.4	93	6.8	7939623	329	7	14	x		R2	*Lycopersicon esculentum*
1650	Xyloglucan endo-transglycosylase/hydrolase (XTH)	30	6.0	31	4.7	57753593	115	2	8	x		R2	*Zea mays*
3161	Putative β-xylosidase	98	5.6	87	5.2	34894432	290	6	6	x		R2	*Oryza sativa*
3163	β-D-xylosidase	69	5.5	83	6.4	18025342	121	2	30	x		R2	*Hordeum vulgare*
3214	β-galactosidase*	32	5.2	84	6.0	61614851	77	2	6		x	R2	*Sandersonia aurantiaca*
3228	Putative α-galactosidase preproprotein*	39	6.6	46	8.1	31432825	210	4	11	x		R2	*Oryza sativa*
3359	Putative β-xylosidase	99	5.7	87	5.2	34894432	213	5	6	x		R2	*Oryza sativa*
3482	β-galactosidase	32	5.0	84	6.0	61614851	70	2	10	x		R2	*Sandersonia aurantia*
3502	β-glucosidase	18	5.6	64	6.2	435313	88	8	11			R2	*Zea mays*
3514	β-glucosidase	55	5.4	64	6.2	435313	109	8	10			MG spot 72	*Zea mays*
3524	β-D-glucosidase	58	5.6	64	6.2	4096602	409	11	24			R2	*Zea mays*

3527	Endo-1,3-1,4-β-D-glucanase	29	7.0	33	7.2	3822036	166	3	13	x		R2	*Zea mays*
	Carbohydrate metabolism												
116	Putative cytosolic 6-phosphogluconate dehydrogenase	52	6.3	53	6.3	3342800	49	2	4	x		R3	*Zea mays*
164	Aldose-1-epimerase-like protein	40	7.1	39	9.4	2739168	335	7	29	x		R1	*Nicotiana tabacum*
409	UDP-glucose pyrophosphorylase*	58	5.2	52	5.5	37729658	521	10	25			R3	*Bambusa oldhamii*
479	Enolase	55	5.3	48	5.2	22273	104	7	23		x	MG spot 81	*Zea mays*
636	Glyceraldehyde-3-phosphate dehydrogenase	39	7.4	36	6.9	34517179	71	2	7			MG spot 30	*Zea mays*
904	UDP-glucose pyrophosphorylase*	28	4.6	52	5.5	37729658	166	3	5			R3	*Bambusa oldhamii*
904	Putative 6-phosphogluconolactonase*	28	4.6	29	5.7	50725145	98	2	7			R3	*Oryza sativa*
918	Triosephosphate isomerase 1*	26	5.2	27	5.7	168647	139	2	9			R3	*Zea mays*
921	Triosephosphate isomerase 1*	26	5.1	27	5.7	168647	139	2	9			R3	*Zea mays*
959	Putative ribose-5-phosphate isomerase*	25	4.3	27	5.1	50934597	108	3	14		x	R3	*Oryza sativa*
1101	UDP-glucose pyrophosphorylase	53	5.5	52	5.5	37729658	140	4	7			R3	*Bambusa oldhamii*
1955	Soluble acid invertase	21	5.8	70	6.4	31872118	270	4	9	x		R3	*Saccharum hybrid cultivar*
1956	Soluble acid invertase	21	5.9	70	6.4	31872118	233	3	9	x		R3	*Saccharum hybrid cultivar*
3228	Fructose bisphosphate aldolase*	39	6.6	46	7.5	295850	210	4	19	x		R2	*Oryza sativa*
3390	Aldose-1-epimerase-like protein*	38	7.6	39	9.4	2739168	198	4	16		x	R2	*Nicotiana tabacum*
3390	Fructose bisphosphate aldolase*	38	7.6	38	7.5	295850	191	4	17			R2	*Zea mays*
3426	Soluble acid invertase	46	5.2	70	6.4	31872118	186	3	6	x		R3	*Saccharum hybrid cultivar*
	Other/unknown												
50	Putative subtilisin-like proteinase*	79	6.1	78	6.3	40538972	47	2	2	x		R1	*Oryza sativa*
53	Putative subtilisin-like proteinase*	78	6.9	78	6.3	40538972	182	4	6	x		R1 R2	*Oryza sativa*

58	Putative subtilisin-like proteinase*	78	6.8	78	6.3	40538972	188	4	6	x		R1	*Oryza sativa*
62	Putative subtilisin-like proteinase*	76	7.4	78	6.3	40538972	129	3	4	x		R1	*Oryza sativa*
74	Putative subtilisin serine protease ARA12*	72	7.7	79	6.3	23296832	132	3	16	x		R1	*Arabidopsis thaliana*
98	Putative β-N-acetylhexosaminidase*	60	6.2	58	6.1	50511452	301	7	14	x		R1	*Oryza sativa*
155	Putative integral membrane Yip1 family protein	42	8.7	40	7.7	34912572	142	3	11	x		R1	*Oryza sativa*
168	α-1,4-glucan-protein synthase	39	5.4	41	6.1	34588146	173	4	10			R1	*Zea mays*
244	Profilin 5*	12	4.5	14	4.7	11493677	68	2	31		x	R1	*Zea mays*
316	Putative r40c1 protein	37	6.7	42	6.7	34902150	252	5	19			R1	*Oryza sativa*
365	Unknown	15	8.2	18	7.8	13194668	110	2	20	x		R3	*Pennisetum cliare*
604	Putative 41 kD chloroplast nucleoid DNA binding protein	43	4.4	54	8.4	50943229	153	3	9	x		R3	*Oryza sativa*
688	Adenosine kinase	39	4.6	36	5.3	4582787	309	6	15			R3	*Zea mays*
855	Putative lipase	31	7.8	38	7.9	55297457	206	4	12	x		R3	*Oryza sativa*
904	Putative carboxypeptidase*	28	4.6	52	5.9	20197951	114	2	5	x		R3	*Arabidopsis thaliana*
920	Putative PS60*	60	6.8	60	8.8	52076641	162	5	7	x		R2	*Oryza sativa*
959	Oxidoreductase NAD-binding domain-containing protein*	25	4.3	30	8.5	42571485	239	5	19		x	R3	*Arabidopsis thaliana*
1020	Translationally controlled tumor protein-like protein	22	4.0	19	4.7	23955914	191	5	38		x	R3	*Zea mays*
1158	Putative ubiquitin-conjugating enzyme family protein	17	6.8	17	6.9	50725506	230	5	38		x	R3	*Oryza sativa*
1334	Profilin 5*	14	4.4	14	4.7	11493677	120	3	33		x	R3	*Zea mays*
1334	Ubiquitin-like protein*	14	4.4	11	5.1	1668773	109	2	25			R3	*Oryza sativa*
1434	Cytochrome b5 domain-containing protein-like	11	4.8	11	5.5	50915542	105	3	28			R3	*Oryza sativa*
1518	Putative leucine aminopeptidase	58	5.4	64	6.5	21206625	366	13	16	x		MG spot 14	*Oryza sativa*
1902	Putative lipase*	34	8.1	38	8.4	55297457	217	4	12	x		R3	*Oryza sativa*
1948	OSJNBb0091E11.17	20	4.6	40	6.1	50925937	100	2	6	x		R3	*Oryza sativa*
3337	Putative lipase	18	5.2	38	7.9	55297457	97	2	5	x		R3	*Oryza sativa*
3385	Putative lipoamide	51	6.4	59	6.5	34894958	150	4	9			R2	*Oryza sativa*

	dehydrogenase												
3420	Putative subtilisin-like proteinase*	76	5.8	78	6.3	40538972	224	3	7	x		R2	*Oryza sativa*
3464	Legumin-like protein*	35	5.9	38	5.8	28950668	173	4	14		x	R2	*Zea mays*
3465	Legumin-like protein*	34	6.0	38	5.8	28950668	179	3	11		x	R2	*Zea mays*
3507	Legumin-like protein	38	6.3	38	5.8	28950668	256	6	23		x	R2	*Zea mays*